AGU PUBLICATIONS

Water Resources Research

RESEARCH ARTICLE
10.1002/2016WR019863

A process-based insight into nonstationarity of the probability distribution of annual runoff

Cong Jiang[1], Lihua Xiong[1], Shenglian Guo[1], Jun Xia[1], and Chong-Yu Xu[1,2]

[1]State Key Laboratory of Water Resources and Hydropower Engineering Science, Wuhan University, Wuhan, China, [2]Department of Geosciences, University of Oslo, Oslo, Norway

Key Points:
- A nonstationary process-based derivation approach is proposed for annual runoff distribution
- Runoff nonstationarity could be due to nonstationarities in different physical processes
- The proposed method can suggest physical causes in annual runoff nonstationarity

Correspondence to:
L. Xiong,
xionglh@whu.edu.cn

Citation:
Jiang, C., L. Xiong, S. Guo, J. Xia, and C.-Y. Xu (2017), A process-based insight into nonstationarity of the probability distribution of annual runoff, *Water Resour. Res.*, *53*, 4214–4235, doi:10.1002/2016WR019863.

Received 28 SEP 2016
Accepted 1 MAY 2017
Accepted article online 8 MAY 2017
Published online 23 MAY 2017

Abstract In this paper, a process-based analytical derivation approach is proposed to perform a nonstationary analysis for annual runoff distribution by taking into account the information of nonstationarities in both hydrological inputs and runoff generation processes. Under the Budyko hypothesis, annual runoff is simulated as a formulation of hydrological inputs (annual precipitation and potential evaporation) using an annual runoff model based on the Fu equation with a parameter *w* accounting for the runoff generation processes. The nonstationarity of the runoff generation process is captured by the dynamic Fu-equation parameter *w*. Then the multivariate joint probability distribution among the hydrological inputs, the Fu-equation parameter *w*, and the runoff model error *k* is constructed based on the nonstationary analysis for both the hydrological inputs and *w*. Finally, the annual runoff distribution is derived by integrating the multivariate joint probability density function. The derived distribution by the process-based analytical derivation approach performs well in fitting distributions of the annual runoffs from both the Yangtze River and Yellow River, China. For most study watersheds in these two basins, the derived annual runoff distributions are found to be nonstationary, due to the nonstationarities in hydrological inputs (mainly potential evaporation) or the Fu-equation parameter *w*.

Plain Language Summary In this paper, a nonstationary process-based analytical derivation approach is proposed to estimate the annual runoff distribution by taking into account information of nonstationarities in both hydrological inputs and runoff generation processes. The annual runoff generation processes are modeled by Fu equation expressing annual runoff as a formulation of the hydrological inputs (annual precipitation and potential evaporation). Based on the nonstationarity identifications of hydrological inputs and the Fu-equation parameter, the annual runoff distribution is derived by integrating the multivariate joint probability density function among the hydrological inputs, the Fu-equation parameter, and the runoff model error. The nonstationary process-based analytical derivation approach is applied to the annual runoff series from the Yangtze River and Yellow River, China, and performs well in fitting annual runoff distributions. This approach is able to provide a process-based insight into the nonstationarity in annual runoff.

1. Introduction

Because of pervasive human activities across the planet and global warming, it is difficult to find a watershed where hydrological systems are not impacted by a variety of natural and human forces, such as climate variability and change, water resources engineering works (e.g., agricultural irrigation, dam construction, and water diversion projects), and land cover/use change (e.g., urbanization and deforestation) [*Blöschl et al.*, 2007; *Merz et al.*, 2012; *Sivapalan et al.*, 2012; *Di Baldassarre et al.*, 2013; *Montanari et al.*, 2013; *Sivapalan and Blöschl*, 2015; *Vogel et al.*, 2015; *McMillan et al.*, 2016; *Kumar et al.*, 2016; *Yan et al.*, 2016]. Although observed changes in hydrological variables such as flooding are not widespread across the globe [*Stocker et al.*, 2013], the so-called nonstationarity has been detected in many runoff series including annual runoff, low flow and flood [*Xiong and Guo*, 2004; *Villarini et al.*, 2009; *Vogel et al.*, 2011; *Hall et al.*, 2014; *Bender et al.*, 2014; *Jiang et al.*, 2015a; *Kim et al.*, 2016]. The basic stationarity assumption in traditional hydrological frequency analysis is being questioned, and therefore nonstationarity is increasingly recognized as a considerable challenge in water resources and flood management,

as well as the design and operation of hydraulic infrastructure [*Salas and Obeysekera*, 2014; *Read and Vogel*, 2016; *Turner and Galelli*, 2016].

In most current literature, identifying whether nonstationarity exists in runoff series is mainly treated as a pure statistical problem, which is then addressed using the trend/change-point tests, such as the Mann-Kendall (MK) test and Spearman test for trends, and Pettitt test for change points [*Mann*, 1945; *Kendall*, 1975; *Pettitt*, 1979; *Yue et al*., 2002; *Burn and Hag Elnur*, 2002; *Xiong and Guo*, 2004; *Vogel et al*., 2013; *Cui and Li*, 2016; *Wei et al*., 2016]. The nonstationarity of runoff series can be modeled by the time-varying moments model, in which the statistical parameters (which can be expressed through moments) of the runoff probability distributions are linked to time, climatic indices, or human activity indices [*Villarini et al*., 2009; *López and Francés*, 2013; *Du et al*., 2015; *Jiang et al*., 2015a]. Both the trend/change-point tests and time-varying moments model are able to provide a primary argument for the nonstationarity of runoff series from statistical perspective, but they are unable to provide a physical insight into how the changes in the hydrological physical mechanisms behind runoff generation will lead to changes in the shape of the runoff frequency curves [*Merz et al*., 2012]. The nonstationarity of runoff series can originate from nonstationarity in hydrological inputs to hydrological systems, or nonstationarity in watershed characteristics dominating processes of runoff generation and routing, or both [*Blöschl and Sivapalan*, 1997; *Merz and Blöschl*, 2009a, 2009b; *Hundecha and Merz*, 2012; *Rogger et al*., 2012a, 2012b, 2013; *Merz et al*., 2015; *Farmer and Vogel*, 2016].

Two different process-based methodologies have been developed to estimate runoff frequency curves by directly considering the hydrological processes involved in runoff generation. The first methodology is the derivation approach based on continuous runoff simulation, where the runoff frequency curve is obtained via a continuous hydrological model driven by rainfall time series that is observed or generated using a stochastic rainfall model [*Blazkova and Beven*, 1997; *Cameron et al*., 2000; *Rahman et al*., 2002]. The second methodology is the process-based analytical derivation approach, which was first outlined by *Eagleson* [1972] and further developed in subsequent studies [*Gottschalk and Weingartner*, 1998; *Fiorentino and Iacobellis*, 2001; *De Michele and Salvadori*, 2002; *Sivapalan et al*., 2005; *Yu et al*., 2014; *Xiong et al*., 2014]. For the process-based analytical derivation approach, the probability distribution of runoff series can be directly derived from the probability distributions of hydrological input variables via a simple hydrological model, which is usually expressed by one or several explicit equations. Compared with the derivation approach based on continuous runoff simulation, the process-based analytical derivation approach may neglect some details in hydrological processes, such as heterogeneity in rainfall or antecedent moisture condition, but has the advantage that the key factors controlling the runoff frequency curve can be clearly presented [*Sivapalan et al*., 2005].

In the study of *Eagleson* [1972] and subsequent studies [*Gottschalk and Weingartner*, 1998; *Fiorentino and Iacobellis*, 2001; *De Michele and Salvadori*, 2002], the process-based analytical derivation approach was applied with an implicit assumption that the simulated runoff values from hydrological models are assumed to be equal to the true runoff values by neglecting model errors. However, no model is perfect, and therefore model errors inherently exist in hydrological simulation [*Montanari and Koutsoyiannis*, 2014]. Both the simulated runoff and the model error should be considered in deriving the runoff distribution [*Farmer and Vogel*, 2016]. *Montanari and Koutsoyiannis* [2012] proposed a blueprint for hydrological uncertainty analysis, where the probability distribution of the true value to be predicted by a hydrological model depends on the joint probability distributions between hydrological input data, model parameters, as well as model uncertainty component (or model error). This blueprint can be simplified into the process-based analytical derivation approach outlined by *Eagleson* [1972], when the parameters of the hydrological model are treated as constant and the model uncertainty component is ignored.

To our knowledge, these two alternative process-based methodologies for deriving runoff frequency curves are usually employed under the stationarity assumption, which means that neither the probability distributions of hydrological input variables nor the adopted hydrological models are allowed to vary with time. However, in reality, the hydrological inputs (such as precipitation and potential evaporation) into hydrological systems would probably be nonstationary [*Cong et al*., 2009; *McMillan et al*., 2016; *Kumar et al*., 2016], and the calibrated parameters in hydrological models have also been found to be nonstationary as they are closely related to changing climatic conditions and land cover [*Merz et al*., 2011; *Westra et al*., 2014; *Jiang et al*., 2015b; *Li et al*., 2015; *Pathiraja et al*., 2016].

In this paper, a nonstationary process-based analytical derivation approach is proposed to provide a physical insight into the effect of the nonstationarities in hydrological processes on the annual runoff probability. For the purpose of considering the effect of runoff simulation error on the derived annual runoff distribution (DARD), this approach is constructed based on the blueprint proposed by *Montanari and Koutsoyiannis* [2012]. Under this approach framework, the DARD depends on the hydrological input variables (including precipitation and potential evaporation), the runoff generation processes characterized by the Fu equation under the Budyko hypothesis [*Budyko*, 1974; *Fu*, 1981; *Zhang et al.*, 2001], as well as the runoff model error. Thus, the nonstationarity sources of the DARD can be clearly identified by analyzing the nonstationarities in both hydrological input variables and the single parameter used in the Fu equation.

The remainder of this paper is organized as follows: in the next section, the methods used in this study are described. In section 3, the proposed approach is applied to the watersheds located in both the Yangtze River basin and Yellow River basin, China. Section 4 contains the discussion. Finally, the main conclusions are summarized in section 5.

2. Methods

2.1. Framework of the Nonstationary Process-Based Analytical Derivation Approach for the Probability Distribution of Runoff

A hydrological model with a mathematical relationship at time t between the observed runoff Q_t ($t=1,2,\ldots,N$, N is the length of the annual runoff series) and the hydrological inputs $\mathbf{y}_t$ can be expressed as

$$Q_t = k_t \cdot \hat{Q}_t = g(\mathbf{y}_t, k_t|\mathbf{w}_t), \tag{1}$$

where $\mathbf{w}_t$ is the vector consisting of the hydrological model parameters and $\hat{Q}_t$ is the simulated runoff with given hydrological inputs $\mathbf{y}_t$ and model parameters $\mathbf{w}_t$. In this study, the model error for the simulated runoff $\hat{Q}_t$ is assumed to be in the multiplicative form and denoted by k_t, which equals to ratio of the observed runoff Q_t to $\hat{Q}_t$, i.e., $Q_t/\hat{Q}_t$.

Assume that the hydrological inputs $\mathbf{y}_t$, the hydrological model parameters $\mathbf{w}_t$, and the model error k_t in runoff simulation are all random variables, the joint probability distribution of $\mathbf{y}_t$, $\mathbf{w}_t$, and k_t can be denoted by the density function of $f_t(\mathbf{y}_t, \mathbf{w}_t, k_t)$. Thus, the probability distribution of runoff Q_t can be derived by integrating $f_t(\mathbf{y}_t, \mathbf{w}_t, k_t)$ over the domain constrained by equation (1) as follows:

$$F_{Q,t}(Q_t) = \iiint_{\Omega: g(\mathbf{y}_t, k_t|\mathbf{w}_t) < Q_t} f_t(\mathbf{y}_t, \mathbf{w}_t, k_t) d\mathbf{y}_t \cdot d\mathbf{w}_t \cdot dk_t. \tag{2}$$

It needs to be emphasized that if the hydrological model has no systematic bias in runoff simulation, the model error k_t is assumed to follow a stationary process, i.e., $k_t \sim F_k(k_t|\boldsymbol{\theta}_k)$, where $\boldsymbol{\theta}_k$ represents the distribution parameters for k_t. Since there is usually no closed-form solution for equation (2), some forms of numerical integration are needed for estimating the derived runoff distribution $F_{Q,t}(Q_t)$.

Compared with the process-based analytical approach outlined by *Eagleson* [1972], equation (2) is a more general framework for deriving the runoff probability distribution because it is able to consider two new factors, one is the hydrological model errors and the other is the nonstationarities in both hydrological inputs and runoff generation processes.

In studying the nonstationarity in the derived runoff probability distribution according to equation (2), there are four different scenarios in terms of nonstationarities in the hydrological inputs and model parameters. The first nonstationarity scenario is that both the hydrological inputs $\mathbf{y}_t$ and model parameters $\mathbf{w}_t$ are nonstationary, and they are denoted as follows:

$$\mathbf{y}_t \sim F_y(\mathbf{y}_t|\boldsymbol{\theta}_{y,t}),\ \mathbf{w}_t \sim F_w(\mathbf{w}_t|\boldsymbol{\theta}_{w,t}), \tag{3}$$

The nonstationarities of both the hydrological inputs and model parameters are modeled by the time variations of their respective distribution parameters, i.e., $\boldsymbol{\theta}_{y,t}$ and $\boldsymbol{\theta}_{w,t}$. The subscript t of the distribution parameters $\boldsymbol{\theta}_{y,t}$ and $\boldsymbol{\theta}_{w,t}$ is used to show that the probability distribution is nonstationary.

The second scenario for equation (2) is that only the hydrological input variables $\mathbf{y}_t$ follow a nonstationary process, while the model parameters $\mathbf{w}_t$ are stationary, namely,

$$\mathbf{y}_t \sim F_y(\mathbf{y}_t|\boldsymbol{\theta}_{y,t}),\ \mathbf{w}_t \sim F_w(\mathbf{w}_t|\boldsymbol{\theta}_w), \tag{4}$$

The third scenario for equation (2) is that only the hydrological inputs $\mathbf{y}_t$ are stationary, while the model parameters $\mathbf{w}_t$ follow a nonstationary process, i.e.,

$$\mathbf{y}_t \sim F_y(\mathbf{y}_t|\boldsymbol{\theta}_y),\ \mathbf{w}_t \sim F_w(\mathbf{w}_t|\boldsymbol{\theta}_{w,t}), \tag{5}$$

The fourth scenario of equation (2) is that both the hydrological inputs $\mathbf{y}_t$ and the model parameters $\mathbf{w}_t$ follow stationary processes, i.e.,

$$\mathbf{y}_t \sim F_y(\mathbf{y}_t|\boldsymbol{\theta}_y),\ \mathbf{w}_t \sim F_w(\mathbf{w}_t|\boldsymbol{\theta}_w), \tag{6}$$

For the fourth scenario, equation (2) can be written as

$$F_Q(Q) = \iiint\limits_{\Omega:g(\mathbf{y},k|\mathbf{w})<Q} f(\mathbf{y},\mathbf{w},k)d\mathbf{y}\cdot d\mathbf{w}\cdot dk, \tag{7}$$

where the stationary hydrological inputs, model parameters, and model multiplicative error are denoted as $\mathbf{y}$, $\mathbf{w}$, and k, respectively. Equation (7) is actually the general form for the process-based analytical derivation approach employed in previous studies under the stationarity assumption [*Eagleson*, 1972; *Gottschalk and Weingartner*, 1998; *Fiorentino and Iacobellis*, 2001; *De Michele and Salvadori*, 2002; *Sivapalan et al*., 2005; *Xiong et al*., 2014].

An additional comment about the model parameters $\mathbf{w}_t$ should be noted when equation (2) is employed. If the model parameters $\mathbf{w}_t$ are constant or time-varying as deterministic functions of some independent variables rather than as random variables, equation (2) can be simplified into

$$F_{Q,t}(Q_t) = \iint\limits_{\Omega:g(\mathbf{y}_t,k_t|\mathbf{w}_t)<Q_t} f_t(\mathbf{y}_t,k_t)d\mathbf{y}_t\cdot dk_t. \tag{8}$$

2.2. Analytical Derivation Approach for Probability Distribution of Annual Runoff Based on the Dynamic Fu Equation

The Budyko hypothesis is usually applicable at the multiyear scale, and the actual mean annual evaporation of a catchment can be estimated from the mean annual precipitation and the mean annual potential evaporation using a series of Budyko-type equations [*Budyko*, 1974; *Fu*, 1981; *Zhang et al*., 2001; *Yang et al*., 2009; *Donohue et al*., 2010; *Wang and Hejazi*, 2011; *Xiong and Guo*, 2012]. According to the water balance equation, the mean annual runoff at the multiyear scale can be generally calculated as the difference between the mean annual precipitation and the actual evaporation, since the catchment water storage change is relatively small and thus can be negligible [*Jiang et al*., 2015b]. However, the Budyko-type equations can still be used with acceptable accuracy to estimate annual runoffs for some watersheds [*Xiong et al*., 2014; *Yu et al*., 2015]. In this study, the annual runoff is simulated as the difference between the annual precipitation and annual actual evaporation, by assuming that the Budyko-type equations can be directly used to estimate actual evaporation at the annual scale, as well as by ignoring the interannual change of catchment water storage in the water balance equation.

In this paper, the Fu equation, one of the widely used Budyko-type equation families that use the parameter w to describe the catchment characteristics and to control the Budyko curve shape [*Fu*, 1981], is employed to construct a simple annual runoff model. The annual runoff at time t ($t=1,2,\ldots,N$) can be simulated from annual precipitation P_t and annual potential evaporation Ep_t by

$$\hat{Q}_t = P_t - \hat{E}_t = P_t - B(P_t, Ep_t|w_t) = P_t - P_t\left[1+\phi_t-(1+\phi_t^{w_t})^{1/w_t}\right] = P_t\left[(1+\phi_t^{w_t})^{1/w_t}-\phi_t\right], \tag{9}$$

where $\hat{Q}_t$ represents the simulated runoff corresponding to the observed annual runoff Q_t, $\hat{E}_t$ is the simulated annual actual evaporation calculated by the dynamic Fu equation using the time-varying parameter w_t, expressed by the term $B(P_t, Ep_t|w_t)$, and ϕ_t denotes the climatic dryness index equal to the ratio of potential evaporation Ep_t to precipitation P_t, i.e., Ep_t/P_t. In equation (9), the increasing w_t will lift the Budyko

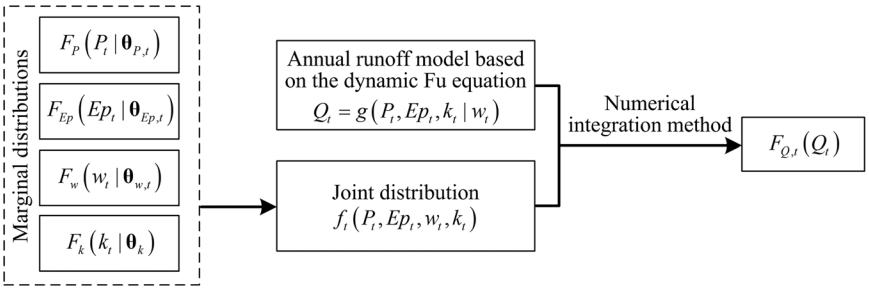

Figure 1. Framework of the analytical approach for deriving the probability distribution of annual runoff based on the dynamic Fu equation.

curve of the catchment and therefore will increase the evaporation ratio E_t/P_t or decrease the runoff ratio Q_t/P_t (and vice versa).

Substituting equation (9) into equation (1) yields the expression of the observed runoff,

$$Q_t = k_t \cdot \hat{Q}_t = k_t\left\{P_t\left[\left(1+\phi_t^{w_t}\right)^{1/w_t} - \phi_t\right]\right\} = g(P_t, Ep_t, k_t|w_t), \tag{10}$$

where the model error k_t could be related to the interannual change of catchment water storage. For further discussions about k_t, readers are referred to section 4.1.

The density function $f_t(P_t, Ep_t, w_t, k_t)$ is defined as the joint probability density distribution between the hydrological inputs (i.e., P_t and Ep_t), the Fu-equation parameter w_t, and the model error k_t. The marginal distributions of $f_t(P_t, Ep_t, w_t, k_t)$ are denoted by $F_P(P_t|\boldsymbol{\theta}_{P,t})$, $F_{Ep}(Ep_t|\boldsymbol{\theta}_{Ep,t})$, $F_w(w_t|\boldsymbol{\theta}_{w,t})$, and $F_k(k_t|\boldsymbol{\theta}_k)$, respectively. According to equation (2), the derived annual runoff distribution (DARD) under the Budyko hypothesis is expressed as

$$F_{Q,t}(Q_t) = \iiiint\limits_{\Omega: g(P_t, Ep_t, k_t|w_t) < Q_t} f_t(P_t, Ep_t, w_t, k_t)\, dP_t \cdot dEp_t \cdot dw_t \cdot dk_t. \tag{11}$$

The framework of the analytical derivation approach for the annual runoff distribution is schematically presented in Figure 1, which contains three steps. Each of these three steps will be detailed in the following sections of 2.3–2.5, respectively. The first step is to construct an annual runoff model based on the dynamic Fu equation. The second step is the estimation of the joint distribution of (P_t,Ep_t,w_t,k_t), including estimating the marginal distributions of $F_P(P_t|\boldsymbol{\theta}_{P,t})$, $F_{Ep}(Ep_t|\boldsymbol{\theta}_{Ep,t})$, $F_w(w_t|\boldsymbol{\theta}_{w,t})$, and $F_k(k_t|\boldsymbol{\theta}_k)$ first, and then constructing the dependence structure of (P_t,Ep_t,w_t,k_t) using the copula method. The third and final step is to estimate the DARD using the numerical integration method.

2.3. Annual Runoff Model Based on the Dynamic Fu Equation

2.3.1. Formulation of the Dynamic Annual Runoff Model

Some previous studies revealed that the parameters in the Budyko-type equations are dominated by certain catchment characteristics such as climatic conditions, and land use and cover [*Zhang et al*., 2001; *Yang et al*., 2009; *Donohue et al*., 2010; *Williams et al*., 2012; *Li et al*., 2013]. These parameters can evolve with changes in both climate and human activities [*Jiang et al*., 2015b]. In order to assess the effects of changes in both climate and human activities on runoff generation processes, the Fu-equation parameter w_t ($t = 1, 2, \ldots, N$) is written as a function of several covariates (denoted as $\mathbf{x}_t$), which include climatic indices (denoted as $\mathbf{x}_{c,t}$) as well as human activity indices (denoted as $\mathbf{x}_{h,t}$), i.e., $\mathbf{x}_t = (\mathrm{x}_{c,t}, \mathbf{x}_{h,t})$. In this paper, climatic covariate indices such as precipitation and temperature are treated as random variables, while human covariate indices such as population and irrigated area are treated as nonrandom variables. If w_t is related to at least one climatic index, it should be a random variable accordingly; otherwise, w_t should be treated as a nonrandom variable or as a constant.

To clearly establish the relationship of the change in w_t with respect to the constant or average parameter $\bar{w}$ to the changes in the covariates with respect to their individual averages, the formulation of w_t is written as

$$\psi(w_t/\bar{w})-\psi(1)=\sum_{i=1}^{m}\alpha_i\left[\varphi_i\left(x_{i,t}/\bar{x}_i\right)-\varphi_i(1)\right]. \tag{12}$$

Rearranging the above equation yields

$$w_t=\pi(\mathbf{x}_t|\bar{w},\boldsymbol{\alpha})=\pi\left(\mathbf{x}_{c,t},\mathbf{x}_{h,t}|\bar{w},\boldsymbol{\alpha}\right)=\bar{w}\cdot\psi^{-1}\left\{\sum_{i=1}^{m}\alpha_i\left[\varphi_i\left(x_{i,t}/\bar{x}_i\right)-\varphi_i(1)\right]+\psi(1)\right\}, \tag{13}$$

where $\boldsymbol{\alpha}=(\alpha_1,\ldots,\alpha_m)$ is the vector of regression parameters. $\mathbf{x}_t=\left(x_{1,t},\ldots,x_{m,t}\right)$ is the covariate vector and $\bar{x}_i$ is the mean value of the covariate $x_{i,t}$ for the whole observation period. $\varphi_i(\cdot)$ $(i=1,2,\ldots,m)$ and $\psi(\cdot)$ stand for transforming functions such as identity (Id), exponential (Ex), and logarithmic (Lo) forms, so that both linear and nonlinear relationships between w_t and $\mathbf{x}_t$ can be described. It is worth noting that the covariate $x_{i,t}$ in equation (12) or equation (13) has been actually standardized by dividing it by its respective mean value $\bar{x}_i$. From equation (13), the Fu-equation parameter w_t will fluctuate around $\bar{w}$ along with the fluctuation in $x_{i,t}$ around $\bar{x}_i$, and thus the nonstationarity of w_t should follow the nonstationarities of the covariates $\mathbf{x}_t$. w_t should be nonstationary if it has at least one covariate that follows a nonstationary process. Conversely, when no covariate is included in equation (13) or all covariates follow stationary processes, w_t is regarded as stationary.

Substituting equation (13) into equation (9), the simulated annual runoff can be expressed as

$$\hat{Q}_t=P_t-B(P_t,Ep_t|w_t)=P_t-B[P_t,Ep_t|\pi(\mathbf{x}_t|\bar{w},\boldsymbol{\alpha})]. \tag{14}$$

2.3.2. Parameter Estimation

According to equation (10), the observed runoff Q_t can be expressed as

$$Q_t=k_t\cdot\hat{Q}_t=e^{\varepsilon_t}\cdot\hat{Q}_t, \tag{15}$$

where the multiplicative model error k_t is written as e^{ε_t}, in which ε_t is actually the difference between the logarithms of the observed runoff and simulated runoff, i.e., $\varepsilon_t=\ln(Q_t)-\ln\left(\hat{Q}_t\right)$. Here we assume that ε_t follows a normal distribution, i.e., $\varepsilon_t\sim N\left(0,\sigma_\varepsilon^2\right)$, and therefore k_t should follow a stationary lognormal distribution, i.e., $k_t\sim LN\left(0,\sigma_\varepsilon^2\right)$. The model parameters (including $\bar{w}$ and $\boldsymbol{\alpha}$) can be estimated by minimizing root mean square error (RMSE) of the log-transformed runoffs, and the maximum likelihood estimation (MLE) of σ_ε is actually the standard deviation of ε_t.

In this study, the annual precipitation P_t, annual mean temperature T_t, and annual potential evaporation Ep_t are used as the candidate climatic covariates for the Fu-equation parameter w_t, i.e., $\mathbf{x}_{c,t}=(P_t,T_t,Ep_t)$. On the basis of covariate analysis for w_t, substituting equation (14) into equation (15), the expression for calculating annual runoff can be generally written as

$$Q_t=k_t\cdot\{P_t-B[P_t,Ep_t|\pi(\mathbf{x}_t|\bar{w},\boldsymbol{\alpha})]\}=g[P_t,Ep_t,k_t|\pi\left(\mathbf{x}_{c,t},\mathbf{x}_{h,t}|\bar{w},\boldsymbol{\alpha}\right)]=g\left(P_t,Ep_t,T_t,k_t,\mathbf{x}_{h,t}|\bar{w},\boldsymbol{\alpha}\right). \tag{16}$$

2.3.3. Model Selection

In this study, we employ the Bayesian Information Criterion (BIC) [*Schwarz*, 1978] to determine the proper explanatory variables for w_t as well as the types of transforming functions $\varphi_i(\cdot)$ $(i=1,2,\ldots,m)$ and $\psi(\cdot)$ in terms of the smallest measure value. The BIC value can be calculated from the density function of the lognormal distribution $LN(0,\sigma_\varepsilon^2)$ for the model error k_t as follows:

$$BIC=-2\sum_{t=1}^{N}\ln f_k(k_t|0,\sigma_\varepsilon^2)+(m+1)\cdot\ln(N), \tag{17}$$

where $f_k(\cdot)$ is the density function of the lognormal distribution for k_t, $\ln(N)$ is the penalty value of BIC, and $m+1$ stand for the total parameter number of equation (13).

2.4. Estimation of the Multivariate Joint Distribution

In deriving the annual runoff distribution as outlined in Figure 1, an essential step is to estimate the joint probability density function $f_t(P_t,Ep_t,w_t,k_t)(t=1,2,\ldots,N)$. According to section 2.3.1, the Fu-equation parameter w_t is determined by the covariates (including $\mathbf{x}_{h,t}$ and $\mathbf{x}_{c,t}=(P_t,T_t,Ep_t)$) of w_t. Incorporating equation (16) into equation (11), the probability distribution of annual runoff is accordingly expressed as

$$F_{Q,t}(Q_t)= \iiiint_{g\left(P_t,Ep_t,T_t,k_t,\mathbf{x}_{h,t}\middle|\bar{w},\boldsymbol{\alpha}\right)<Q_t} f_t(P_t,Ep_t,T_t,k_t)dP_t\cdot dEp_t\cdot dT_t\cdot dk_t, \tag{18}$$

where the human covariates $\mathbf{x}_{h,t}$ are not treated as the integration variables, because they are considered as deterministic and not random covariates. Thus, to derive the distribution of Q_t, we merely need to construct the joint distribution of (P_t,Ep_t,T_t,k_t) instead of that of (P_t,Ep_t,w_t,k_t). To obtain the joint distribution $f_t(P_t,Ep_t,T_t,k_t)$, the first step is to estimate the nonstationary marginal distributions for (P_t,Ep_t,T_t,k_t). It is known that the probability distribution $F_k(k_t|\boldsymbol{\theta}_k)$ for k_t is the stationary lognormal distribution $LN(0,\sigma_\varepsilon^2)$ as estimated in section 2.3. The nonstationary marginal distributions $F_P\left(P_t|\boldsymbol{\theta}_{P,t}\right)$, $F_{Ep}\left(Ep_t|\boldsymbol{\theta}_{Ep,t}\right)$, and $F_T\left(T_t|\boldsymbol{\theta}_{T,t}\right)$ for the series P_t, Ep_t, and T_t, are estimated using the time-varying moments model. The next step is to construct the dependence structure of (P_t,Ep_t,T_t,k_t) using the copula method on the basis of the marginal distribution estimations.

2.4.1. Estimation of the Nonstationary Marginal Distributions by Using the Time-Varying Moments Model

The nonstationarities of the climatic indices (including P_t, Ep_t, and T_t) are preliminarily examined using the Mann-Kendall trend test [*Mann*, 1945; *Kendall*, 1975] and Pettitt change-point test [*Pettitt*, 1979]. To model the nonstationarities of P_t, Ep_t, and T_t, we need to choose proper distribution functions to fit their probability distributions $F_P\left(P_t|\boldsymbol{\theta}_{P,t}\right)$, $F_{Ep}\left(Ep_t|\boldsymbol{\theta}_{Ep,t}\right)$, and $F_T\left(T_t|\boldsymbol{\theta}_{T,t}\right)$, respectively. Three widely used probability distributions in hydrology, namely, the three-parameter Pearson type III distribution, two-parameter gamma distribution, and two-parameter lognormal distribution [*Villarini et al*., 2009; *Jiang et al*., 2015a], are considered to be the candidate distributions for P_t and Ep_t. The best distribution for fitting both P_t and Ep_t is chosen from these three candidate distributions via BIC. The temperature series T_t is assumed to be normally distributed.

The nonstationarities of P_t, Ep_t, and T_t can be described by the time variations of the distribution parameters $\boldsymbol{\theta}_{P,t}$, $\boldsymbol{\theta}_{Ep,t}$, and $\boldsymbol{\theta}_{T,t}$, respectively. In this study, only the nonstationarity of the first moment parameter (denoted by μ_t) in the distribution is considered and assumed to be in form of trend or change point. Then, the trend or change point in μ_t is described by the time-varying moments model [*Strupczewski et al*., 2001]. Specifically, if the MK trend test indicates a trend at the 0.05 significance level, μ_t is expressed as a function of time t. Three candidate trend models are given as follows:

$$\text{Linear (Li)}: \mu_t=a+bt, \tag{19a}$$

$$\text{Exponential(Ex)}: \mu_t=\exp(a+bt), \tag{19b}$$

$$\text{Logarithmic (Lo)}: \mu_t=a+b\ln t. \tag{19c}$$

If the Pettitt test indicates a significant change point (denoted as cp) at the 0.05 significance level, μ_t is written as

$$\mu_t=\begin{cases}\mu_0 & 1\le t\le cp\\ \mu_0+\Delta\mu & cp<t\le N\end{cases}, \tag{20}$$

where μ_0 is the first moment parameter before the change point cp, $\Delta\mu$ is the abrupt change value of the first moment parameter at cp, and the first moment parameter after cp is therefore $\mu_0+\Delta\mu$.

The parameters of the time-varying moments model are estimated using the MLE method [*Strupczewski et al*., 2001]. The goodness of fit (GOF) of the distributions is examined by the Kolmogorov-Smirnov (KS) test [*Frank and Massey*, 1951]. Finally, the best model for fitting the time-variation in the first moment parameter of the marginal distributions is selected from the stationary model and the four nonstationary models (as expressed by equations (19) and (20)) in terms of the smallest BIC value [*Schwarz*, 1978].

2.4.2. Construction of Multivariate Dependence Structure Using the Pair Copula

Copula method is a very effective and popular tool to describe the dependence structure of multiple random variables with flexible marginal distributions [*Nelsen*, 2006]. On the basis of the marginal distribution estimations, the joint distribution of (P_t,Ep_t,T_t,k_t) can be expressed via a copula function $C(\cdot)$ as follows:

$$F_t(P_t, Ep_t, T_t, k_t) = C\left\{F_P\left(P_t|\boldsymbol{\theta}_{P,t}\right), F_{Ep}\left(Ep_t|\boldsymbol{\theta}_{Ep,t}\right), F_T\left(T_t|\boldsymbol{\theta}_{T,t}\right), F_k(k_t|\boldsymbol{\theta}_k)|\boldsymbol{\theta}_c\right\}, \tag{21}$$

where $\boldsymbol{\theta}_c$ denotes the copula parameters representing the dependence strength of (P_t,Ep_t,T_t,k_t). The density function corresponding to equation (21) is given by

$$\begin{aligned} f_t(P_t, Ep_t, T_t, k_t) = c\left\{F_P\left(P_t|\boldsymbol{\theta}_{P,t}\right), F_{Ep}\left(Ep_t|\boldsymbol{\theta}_{Ep,t}\right), F_T\left(T_t|\boldsymbol{\theta}_{T,t}\right), F_k(k_t|\boldsymbol{\theta}_k)|\boldsymbol{\theta}_c\right\} \\ \cdot f_P\left(P_t|\boldsymbol{\theta}_{P,t}\right) \cdot f_{Ep}\left(Ep_t|\boldsymbol{\theta}_{Ep,t}\right) \cdot f_T\left(T_t|\boldsymbol{\theta}_{T,t}\right) \cdot f_k(k_t|\boldsymbol{\theta}_k) \end{aligned}, \tag{22}$$

where $c(\cdot)$, $f_P(\cdot)$, $f_{Ep}(\cdot)$, $f_T(\cdot)$, and $f_k(\cdot)$ denote the density functions of $C(\cdot)$, $F_P(\cdot)$, $F_{Ep}(\cdot)$, $F_T(\cdot)$, and $F_k(\cdot)$, respectively. It should be noted that the dependence structure of (P_t,Ep_t,T_t,k_t) could be nonstationary [*Bender et al*., 2014; *Jiang et al*., 2015a; *Xiong et al*., 2015], but in this study we prefer to assume a stationary dependence structure, that is, $\boldsymbol{\theta}_c$ is constant for the whole observation period.

Since most of the applied copula functions are for bivariate variables, the dependence structure of (P_t,Ep_t,T_t,k_t) is constructed by the pair copula in form of the canonical vine (C-vine) structure with P_t chosen as the dominant variable [*Aas et al*., 2009; *Xiong et al*., 2014]. Given that annual precipitation and annual potential evaporation are usually negatively correlated [*Xiong et al*., 2014], the Frank copula function and Gaussian copula function, both of which are able to describe positive and negative bivariate dependence structure [*Nelsen*, 2006], are employed as the candidates for composing C-vine copula. The parameters of C-vine copula are estimated using the MLE method [*Aas et al*., 2009]. The copula function with the best fitting quality is determined by BIC, and the goodness-of-fit test for C-vine copula is performed using the Probability Integral Transform (PIT) test [*Aas et al*., 2009].

2.5. Computation and Assessment of the Derived Annual Runoff Distribution

The derived annual runoff distribution (DARD) $F_{Q,t}(\cdot)$ can be computed using the Monte Carlo (MC) sampling technique for evaluating the multiple integral in equation (18) [*Xiong et al*., 2014]. First, generate random samples of (P,Ep,T,k) with the size of N_s according to the joint distribution estimated in section 2.4. Then compute the random runoff samples, which are denoted by $\mathbf{Q}_t^s = \left(Q_{t,1}^s, Q_{t,2}^s, \ldots, Q_{t,N_s}^s\right)$, from random samples of (P,Ep,T,k) using the annual runoff model constructed in section 2.3. Finally, the cumulative probability function (CDF) of the annual runoff variable Q at any time t can be estimated with respect to the generated random samples $\mathbf{Q}_t^s$ using the empirical distribution function,

$$F_{Q,t}(Q) = \frac{1}{N_s+1}\sum_{j=1}^{N_s} \mathbf{1}\left(Q_{t,j}^s \le Q\right). \tag{23}$$

The statistical parameters such as mean and coefficient of variation (Cv) of $F_{Q,t}(\cdot)$ can be estimated from $\mathbf{Q}_t^s$ using the moment method. Using equation (23), the probability of the observed annual runoff Q_t, denoted by p_{Q_t}, can be then estimated. The goodness of fit of $F_{Q,t}(\cdot)$ is assessed by examining whether the estimated probability p_{Q_t} of Q_t is uniformly distributed on the [0, 1] interval by using the KS test at the 0.05 significance level.

3. Applications in the Yangtze River Basin and Yellow River Basin

3.1. Study Area and Data Set

3.1.1. The Yangtze River and Yellow River Basins

In this study, the nonstationary process-based analytical derivation approach will be employed the watersheds located in the Yangtze River and Yellow River, China (Figure 2). The Yangtze River is the largest river in China with a drainage area of 1.8×10^6 km^2 and flow distance of 6300 km. The Yellow River, which ranks second only to the Yangtze River, has a drainage area of 0.75×10^6 km^2 and a length of 5464 km. In recent decades, some detectable changes have been found in runoffs as well as climatic indices such as the temperature and potential evaporation of these two basins [*Xiong and Guo*, 2004; *Cong et al*., 2009; *Zhang et al*., 2011; *Du et al*., 2015]. Both the Yangtze River basin and Yellow River basin play the crucial roles in the society and economy of China. With the rapid development of China in recent decades, the natural hydrological systems of these two rivers should have been in varying degrees disturbed by human activities, such as agriculture irrigation and urbanization [*Zhang et al*., 2011; *Jiang et al*., 2015a, 2015b].

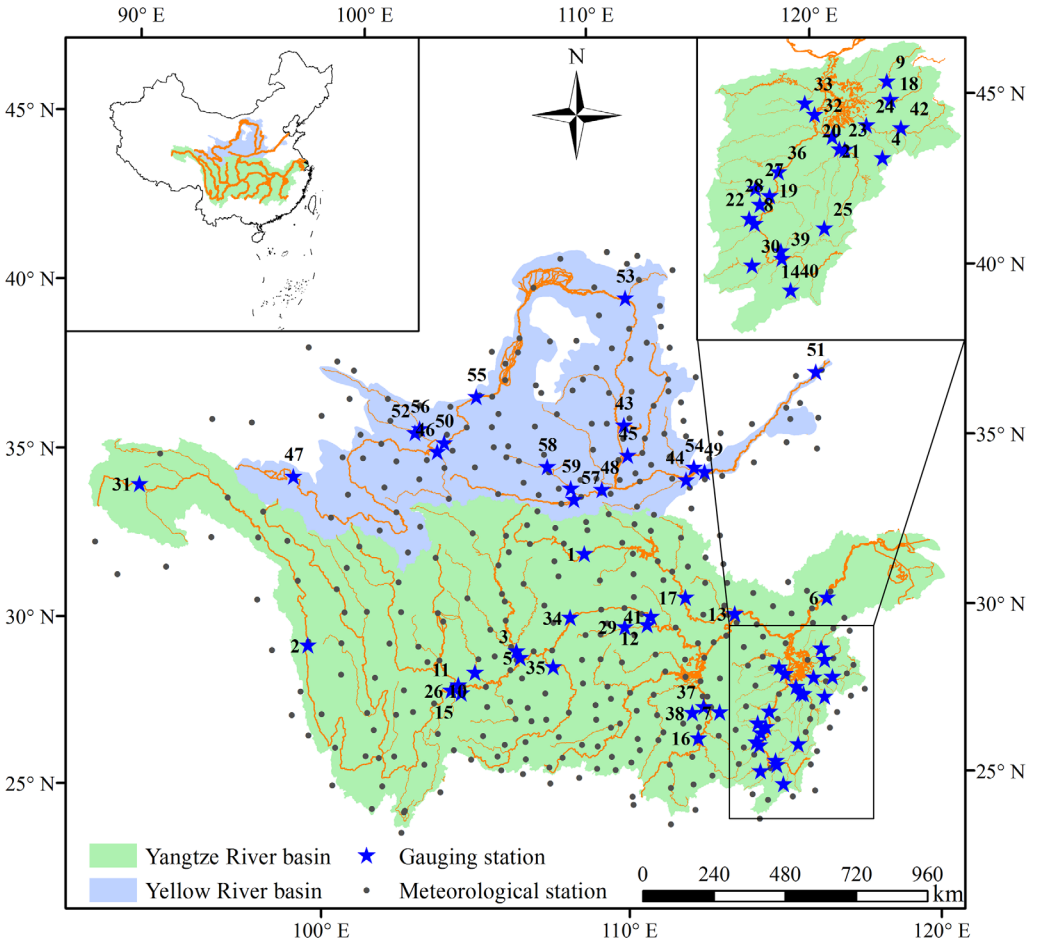

Figure 2. Map of the Yangtze River basin and Yellow River basin.

3.1.2. Data

To perform the case study, the long-term annual runoff series (Q) from a total of 59 watersheds have been gathered, among which 42 watersheds are from the Yangtze River basin and the remaining 17 watersheds are from the Yellow River basin. The spatial distribution of the gauging stations is presented in Figure 2, and the information on the runoff series such as the observation period and drainage area of each gauging station is displayed in Table 1. There are a total of 367 meteorological stations located in and around these two basins. The annual precipitation (P), annual potential evaporation (Ep), and annual mean temperature (T) for each watershed are calculated from the daily observation data, which are obtained from a varying number of meteorological stations within and around the watershed using the Thiessen polygon method.

The effects of human activities on runoff generation are quantified by four indices: population (*Pop*), gross domestic product (*GDP*), irrigated area (*IA*), and grain production (*GP*), which can be used as the indicative factors of human force impacting the hydrological system of a watershed [*Zhang et al.*, 2011; *Jiang et al.*, 2015b]. These four indices will be employed as the candidate explanatory variables for describing the evolution of the Fu-equation parameter w. Since the human activity data at the watershed scale are unavailable, the annual data of *Pop*, *GDP*, *IA*, and *GP* for each watershed are represented by the data of the province(s) where the watershed is located. Specifically, if watershed A is located in provinces B and C, the human activity data for A is represented by the sum of the data for both B and C. The annual data of *Pop*, *GDP*, *IA*, and *GP* for each province in China can be obtained from the book of China Compendium of Statistics 1949–2008 [*Department of Comprehensive Statistics of National Bureau of Statistics*, 2010] and website of the National Bureau of Statistics of the People's Republic of China (http://www.stats.gov.cn/tjsj/ndsj/).

Table 1. Information of the Study Watersheds

ID	Watershed	Observation Period	Area (km^2)
Yangtze River			
1	Ankang	1955–2011	38,600
2	Batang	1960–2012	180,054
3	Beibei	1955–2012	156,736
4	Boquan	1963–2013	553
5	Cuntan	1955–2013	866,559
6	Datong	1955–2012	1,705,383
7	Daxitan	1959–2008	3,132
8	Dongbei	1957–2013	40,231
9	Dufengkeng	1955–2013	5,013
10	Fushun	1955–2012	19,613
11	Gaochang	1955–2012	135,378
12	Geheyan	1955–2009	14,430
13	Hankou	1955–2012	1,488,036
14	Hanlinqiao	1957–2013	2,689
15	Hengjiang	1964–2009	14,781
16	Hengyang	1959–2008	52,150
17	Huangzhuang	1955–2013	142,056
18	Hushan	1955–2013	6,374
19	Jian	1964–2013	56,223
20	Liaojiawan	1955–2013	8,723
21	Lijiadu	1955–2013	15,811
22	Linkeng	1959–2013	994
23	Loujiacun	1955–2013	4,969
24	Meigang	1955–2013	15,535
25	Ningdu	1959–2013	2,372
26	Pingshan	1955–2010	485,099
27	Saitang	1957–2012	3,004
28	Shangshalan	1957–2013	5,257
29	Shuibuya	1955–2009	10,860
30	Tiantou	1958–2013	3,209
31	Tuotuohe	1956–2012	19,742
32	Waizhou	1955–2013	80,948
33	Wanjiabu	1955–2013	3,548
34	Wanxian	1955–2013	974,881
35	Wulong	1955–2013	83,035
36	Xiajiang	1957–2013	62,724
37	Xiangtan	1959–2008	81,638
38	Xiangxiang	1959–2008	6,053
39	Xiashan	1957–2013	16,033
40	Yangxinjiang	1958–2013	569
41	Yichang	1955–2013	1,000,550
42	Yiyang	1957–2013	8,753
Yellow River			
43	Daning	1955–2008	3,992
44	Heishiguan	1955–2013	18,563
45	Hejin	1955–2013	38,728
46	Hongqi	1957–2012	24,973
47	Huangheyan	1957–2012	20,930
48	Huaxian	1955–2013	106,498
49	Huayuankou	1955–2013	730,036
50	Lanzhou	1955–2013	222,551
51	Lijin	1955–2013	751,869
52	Minhe	1955–2013	15,342
53	Toudaoguai	1955–2013	367,898
54	Wuzhi	1956–2013	12,880
55	Xiaheyan	1955–2013	254,142
56	Xiangtang	1955–2013	15,126
57	Xianyang	1955–2009	46,827
58	Yangjiaping	1956–2014	14,126
59	Zhangjiashan	1955–2013	43,216

3.2. Covariate Analysis for the Fu-Equation Parameter *w*

To model the nonstationarity in runoff generation processes related to the changes in watershed characteristics, a covariate analysis for the Fu-equation parameter w is performed by introducing indices of *Pop*, *GDP*, *IA*, *GP*, *P*, *Ep*, and *T* as the candidate explanatory variables of w. The results of covariate analysis have been summarized in Table 2. In terms of both BIC and Nash-Sutcliffe efficiency [*Nash and Sutcliffe*, 1970] of the log-transformed runoff, introducing covariates to consider the time-variation in w is able to significantly improve the performance of the annual runoff model, especially for those watersheds in the Yellow River basin (see Figure 3).

As presented in Table 2, the Fu-equation parameter w for all study watersheds in the Yellow River basin is found to be related to human activity indices. By contrast, w is linked to the human activity indices only for 16 out of the 42 study watersheds in the Yangtze River basin. In general, human activities seem to have the more visible influence on the natural hydrological processes of the Yellow River basin, although the population density, urbanization degree, and agricultural development level in this basin are all generally lower than those in the Yangtze basin. The reason for this is that the hydrological systems in the arid Yellow River basin should be more sensitive to human activities than those in the humid Yangtze River basin [*Zhang et al*., 2011].

The regression coefficient for each covariate of w has been summarized in Figure 4. In most cases, w is positively related to human activity indices, precipitation, and temperature, but negatively related to potential evaporation. Therefore, the more intensive human activities and higher temperature would usually lead to a higher evaporation ratio (i.e., E/P) or a lower runoff ratio (i.e., Q/P). The precipitation rise can lead to the increase of the runoff via directly increasing the water supply to the watershed. But meanwhile, the positive relationship between w and precipitation indicates that the precipitation increase would also increase the evaporation ratio by lifting the Budyko curve and partially offset the direct effect of the water supply growth. Similar to precipitation, potential evaporation

Table 2. Summary of the Results of Covariate Analysis for the Fu-Equation Parameter w in the Annual Runoff Model[a]

ID	Catchment	Covariates of w	Transforming Function $\psi(\cdot)$ of w	BIC of the Annual Runoff Model	
				Constant w	Nonconstant w
Yangtze River					
1	Ankang	Pop^{Id}	Logarithmic	−74.55	−93.31
2	Batang	Pop^{Lo},Ep^{Id},T^{Ex}	Exponential	−61.92	−69.61
3	Beibei	Pop^{Ex},IA^{Ex},T^{Lo}	Exponential	−119.17	−131.53
4	Boquan	P^{Lo}	Exponential	−49.80	−50.13
5	Cuntan	GP^{Lo},IA^{Lo},Ep^{Id}	Exponential	−180.91	−192.97
6	Datong			−170.49	
7	Daxitan	GP^{Lo},P^{Ex}	Logarithmic	−50.89	−51.25
8	Dongbei			−58.72	
9	Dufengkeng			−32.05	
10	Fushun			−48.29	
11	Gaochang	GP^{Lo},P^{Lo},Ep^{Id}	Logarithmic	−159.11	−169.09
12	Geheyan	Pop^{Ex},GP^{Lo},Ep^{Id}	Linear	−84.66	−108.37
13	Hankou			−192.18	
14	Hanlinqiao			−47.40	
15	Hengjiang	Pop^{Lo}	Exponential	−51.99	−53.53
16	Hengyang	Pop^{Ex},P^{Lo}	Exponential	−51.78	−56.17
17	Huangzhuang	Pop^{Lo}	Logarithmic	−17.57	−28.76
18	Hushan			−50.81	
19	Ji'an	Pop^{Lo},GP^{Id},Ep^{Id}	Logarithmic	−55.54	−68.95
20	Liaojiawan	Pop^{Ex},GP^{Ex},Ep^{Id}	Logarithmic	−35.99	−45.62
21	Lijiadu	GP^{Id}	Exponential	−8.72	−13.51
22	Linkeng			−17.60	
23	Loujiacun	Pop^{Ex}	Exponential	−61.15	−61.53
24	Meigang			−98.70	
25	Ningdu			−45.79	
26	Pingshan			−131.29	
27	Saitang			−38.87	
28	Shangshalan			−31.44	
29	Shuibuya	Pop^{Ex},GP^{Lo},Ep^{Id}	Identity	−82.53	−104.59
30	Tiantou			−18.57	
31	Tuotuohe	P^{Id},T^{Id}	Logarithmic	45.91	27.86
32	Waizhou			−74.38	
33	Wanjiabu	Ep^{Id}	Logarithmic	−32.17	−32.19
34	Wanxian	T^{Ex}	Logarithmic	−172.16	−180.20
35	Wulong	P^{Lo}	Exponential	−146.49	−148.84
36	Xiajiang			−57.69	
37	Xiangtan	Pop^{Ex},P^{Ex}	Logarithmic	−48.71	−52.93
38	Xiangxiang			5.16	
39	Xiashan			−47.45	
40	Yangxinjiang	Ep^{Id},T^{Id}	Logarithmic	−4.68	−8.73
41	Yichang	T^{Ex}	Logarithmic	−184.17	−188.02
42	Yiyang	Ep^{Id}	Logarithmic	−94.28	−96.09
Yellow River					
43	Daning	Pop^{Id},P^{Ex},Ep^{Id}	Logarithmic	80.80	21.71
44	Heishiguan	Pop^{Ex},P^{Id},Ep^{Id}	Identity	84.53	46.85
45	Hejin	Pop^{Id},IA^{Lo},P^{Lo}	Logarithmic	129.07	61.59
46	Hongqi	Pop^{Lo},IA^{Id}	Logarithmic	−44.58	−54.50
47	Huangheyan	GDP^{Id}	Exponential	149.10	139.83
48	Huaxian	Pop^{Lo},Ep^{Id}	Identity	38.27	14.71
49	Huayuankou	IA^{Id},P^{Ex}	Exponential	44.05	−12.30
50	Lanzhou	Pop^{Lo},IA^{Lo},P^{Id}	Logarithmic	−30.20	−56.15
51	Lijin	Pop^{Id}	Exponential	121.87	72.42
52	Minhe	Pop^{Id},P^{Lo}	Logarithmic	16.76	−27.52
53	Toudaoguai	GP^{Lo},P^{Ex}	Identity	36.67	5.41
54	Wuzhi	IA^{Lo},GP^{Ex},Ep^{Id}	Exponential	151.06	107.03
55	Xiaheyan	Pop^{Lo},IA^{Lo},P^{Ex}	Logarithmic	−17.35	−52.11
56	Xiangtang	IA^{Lo},P^{Id}	Identity	−43.41	−83.96
57	Xianyang	Pop^{Id}	Exponential	89.77	67.42
58	Yangjiaping	GP^{Id}	Exponential	72.15	57.37
59	Zhangjiashan	GP^{Id}	Exponential	91.09	90.62

[a]The superscripts "Id," "Ex," and "Lo" indicate that the chosen transforming functions $\varphi_i(\cdot)$ for the covariates of w in equation (13) are identity, exponential, and logarithmic, respectively.

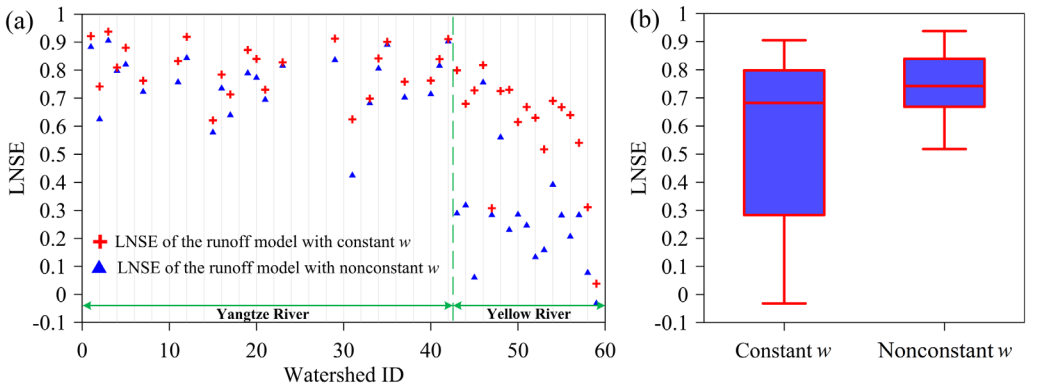

Figure 3. Performance comparison of the annual runoff models. (a) The performance comparison for each individual watershed; (b) the comparison of the overall performance of annual runoff models.

change would also have both positive and negative effects on runoff. In particular, the decrease of potential evaporation can lead to the increase of runoff via directly reducing energy supply to watershed, but would also increase the evaporation ratio by lifting the Budyko curve, and then partially offset the direct effect of the energy supply reduction. These findings indicate that climate change can impact runoff in two ways: one is to change the hydrological inputs into the watershed system, and the other is to alter the runoff generation processes represented by the Budyko curve shape.

3.3. Estimation of the Multivariate Joint Probability Distribution of (*P,Ep,T,k*)

3.3.1. Estimation of the Marginal Distributions for (*P,Ep,T,k*)

Both the Mann-Kendall trend test and Pettitt change-point test are used to examine the nonstationarities of the annual runoff *Q*, annual precipitation *P*, annual potential evaporation *Ep*, and annual average temperature *T* of each watershed in the Yangtze and Yellow River basins. As shown in Figure 5, most runoff series in the Yangtze River basin have neither significant trends nor change points, while the majority of the runoff series in the Yellow River basin present significant downward trends as well as change points. The results of the trend/change-point tests indicate that precipitation series have significant trends and/or change points in only a few watersheds, while significant downward trends and/or change points are detected in potential evaporation series for most watersheds. Synchronized with global warming trends, annual temperature in all study watersheds has been detected with significant upward trends and/or change points. The fact that the potential evaporation series and the temperature series have the opposite trends is actually the so-called evaporation paradox phenomenon, which has been widely observed in China [*Xu et al.*, 2006; *Cong et al.*, 2009].

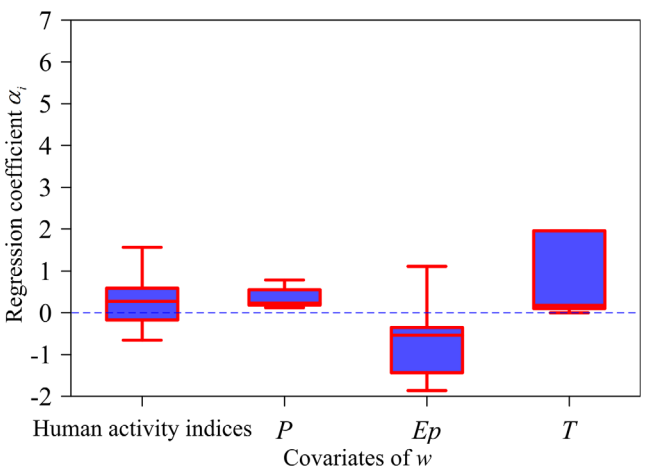

Figure 4. Regression coefficient α_i ($i=1,2,\ldots,m$) in equation (13) for each covariate of the Fu-equation parameter *w*.

Based on the results of the trend/change-point tests for the meteorological series, the marginal distributions of *P*, *Ep*, and *T* (if *T* is a covariate of *w*) are estimated using the time-varying moments model. The specific nonstationarity type and the BIC value for each nonstationary marginal distribution have been summarized in Table 3. Figure 6 indicates that marginal distributions for all meteorological series have a satisfactory fitting effect by passing the KS test at the 0.05 significance level. From the results of the KS test shown in Figure 6, the log-normal distribution $LN(0,\sigma_\varepsilon^2)$ can satisfactorily fit the model error *k* for the majority of the study watersheds.

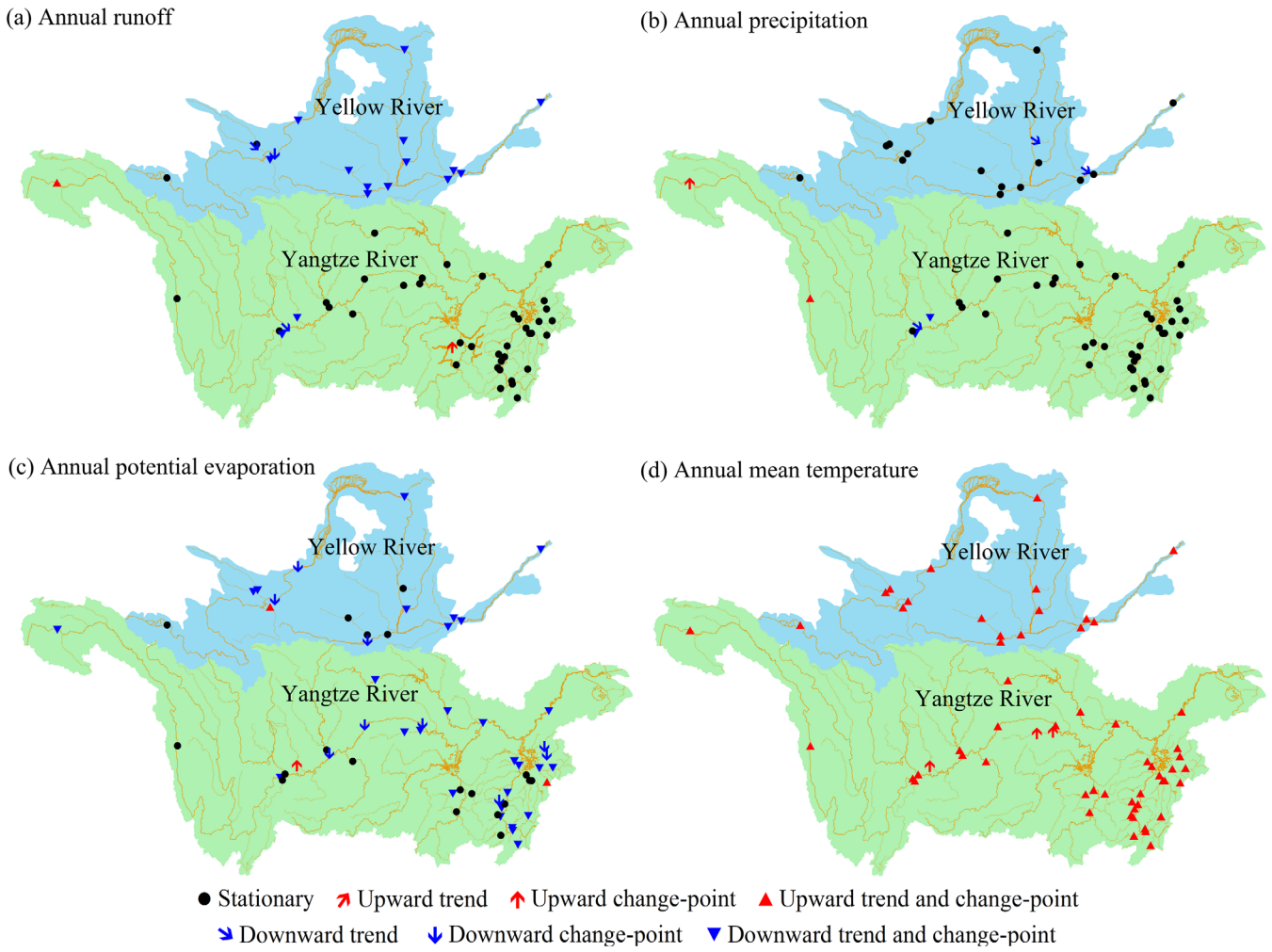

Figure 5. Trend/change-point tests for the hydro-meteorological series in the Yangtze and Yellow River basins.

3.3.2. Construction of the Dependence Structure for (*P,Ep,T,k*)

The dependence structure between *P*, *Ep*, *T* (if *T* is a covariate of *w*), and *k* is constructed using the C-vine pair copula with *P* as the dominant variable. The results indicate that the dependences of the pairs of both (*P*,*Ep*) and (*P*,*T*) are always negative, while the dependences of (*P*,*k*) can be either positive or negative. The results of the PIT test for the constructed C-vine copulas have been displayed in Figure 6. The *p* values of the PIT test for the copulas are generally larger than the significance level of 0.05. Consequently, the C-vine copula is able to satisfactorily describe the dependence structure of *P*, *Ep*, *T* (if *T* is a covariate of *w*), and *k* for the vast majority of the study watersheds.

3.4. The Estimation of the Derived Annual Runoff Distribution

After the annual runoff model based on the dynamic Fu equation is established, i.e., equation (16), as well as the joint probability distribution between *P*, *Ep*, *T* (if *T* is a covariate of *w*), and *k* are identified by equation (22), the Monte Carlo sampling method with 10,000 samples is used to estimate the derived annual runoff distribution (DARD) as explained in section 2.5. Then the probability of the observed annual runoff can be estimated by using the empirical distribution function as shown in equation (23). The goodness-of-fit test shows that the DARD has a satisfactory performance in fitting the annual runoff distributions of almost all watersheds (Figure 6).

Figure 7 compares the linear trends of the mean of the DARD and the observed annual runoff for each study watershed. In order to remove the effect of runoff magnitude, both of two trends have been standardized by

Table 3. Summary of the Results of Nonstationary Marginal Distribution Estimations for the Meteorological Series Using the Time-Varying Moments Model[a]

		Nonstationarity Type			BIC of Stationary Model			BIC of Nonstationary Model		
ID	Catchment	*P*	*Ep*	*T*	*P*	*Ep*	*T*	*P*	*Ep*	*T*
Yangtze River										
1	Ankang	St	CP		746.58	657.58			639.13	
2	Batang	CP	St	CP	566.13	583.88	119.07	559.66		85.37
3	Beibei	St	St	CP	716.31	645.11	65.44			39.75
4	Boquan	St	CP		764.79	642.80			624.47	
5	Cuntan	St	CP		625.60	611.77			605.89	
6	Datong	St	CP		663.75	603.01			586.63	
7	Daxitan	St	St		689.61	588.30				
8	Dongbei	St	CP		807.92	670.35			650.80	
9	Dufengkeng	St	CP		856.51	701.43			692.43	
10	Fushun	Tr^{Ex}	CP		737.91	648.30		729.61	639.09	
11	Gaochang	Tr^{Li}	St		660.98	606.83		660.12		
12	Geheyan	St	Tr^{Lo}		750.52	634.72			613.84	
13	Hankou	St	CP		638.01	599.38			586.32	
14	Hanlinqiao	St	CP		821.81	703.70			675.98	
15	Hengjiang	CP	St		557.07	513.01		548.46		
16	Hengyang	St	St		690.32	573.20				
17	Huangzhuang	St	CP		749.23	687.68			665.14	
18	Hushan	St	CP		868.13	691.98			678.02	
19	Ji'an	St	St		703.16	577.06				
20	Liaojiawan	St	St		859.01	726.91				
21	Lijiadu	St	St		855.07	724.57				
22	Linkeng	St	St		797.58	636.16				
23	Loujiacun	St	St		853.22	713.93				
24	Meigang	St	CP		863.73	694.14			680.04	
25	Ningdu	St	CP		810.64	676.97			644.71	
26	Pingshan	St	CP		601.34	606.88			600.79	
27	Saitang	St	CP		788.35	668.08			652.31	
28	Shangshalan	St	Tr^{Lo}		813.28	662.83			654.16	
29	Shuibuya	St	Tr^{Lo}		753.67	634.34			617.82	
30	Tiantou	St	St		791.53	638.55				
31	Tuotuohe	CP	Tr^{Lo}	CP	642.18	679.66	149.81	633.93	670.12	124.59
32	Waizhou	St	CP		821.36	691.99			669.21	
33	Wanjiabu	St	CP		838.73	732.48			690.54	
34	Wanxian	St	CP	CP	624.30	610.83	80.62		604.50	39.29
35	Wulong	St	St		743.76	640.84				
36	Xiajiang	St	CP		804.55	668.95			650.99	
37	Xiangtan	St	St		687.45	570.40				
38	Xiangxiang	St	CP		678.25	605.41			588.42	
39	Xiashan	St	CP		816.95	683.52			654.57	
40	Yangxinjiang	St	Tr^{Lo}	CP	813.07	697.97	44.84		688.68	32.00
41	Yichang	St	CP	CP	626.14	611.19	79.68		603.45	38.92
42	Yiyang	St	CP		836.96	663.72			654.27	
Yellow River										
43	Daning	Tr^{Ex}	St		669.88	648.19		666.88		
44	Heishiguan	St	CP		753.54	739.71			696.06	
45	Hejin	St	CP		711.74	699.15			688.32	
46	Hongqi	St	CP		651.69	609.88			590.90	
47	Huangheyan	St	St		608.50	632.08				
48	Huaxian	St	St		706.48	697.12				
49	Huayuankou	St	CP		651.47	666.00			639.78	
50	Lanzhou	St	CP		634.64	644.12			639.20	
51	Lijin	St	CP		650.89	666.77			637.40	
52	Minhe	St	CP		659.89	705.44			662.75	
53	Toudaoguai	St	CP		622.76	655.03			622.94	
54	Wuzhi	St	CP		721.19	708.31			687.45	
55	Xiaheyan	St	CP		628.99	651.72			642.86	
56	Xiangtang	St	Tr^{Lo}		632.91	665.83			633.85	
57	Xianyang	St	CP		662.57	646.63			632.34	
58	Yangjiaping	St	St		717.10	702.42				
59	Zhangjiashan	St	St		710.59	706.92				

[a]The symbol "St" indicates that the series is stationary, while "Tr" and "CP" demonstrate that the series have significant trends and change points, respectively. The superscripts "Li," "Ex," and "Lo" indicate that the selected trend models for the meteorological series are linear, exponential, and logarithmic as in equation (19), respectively.

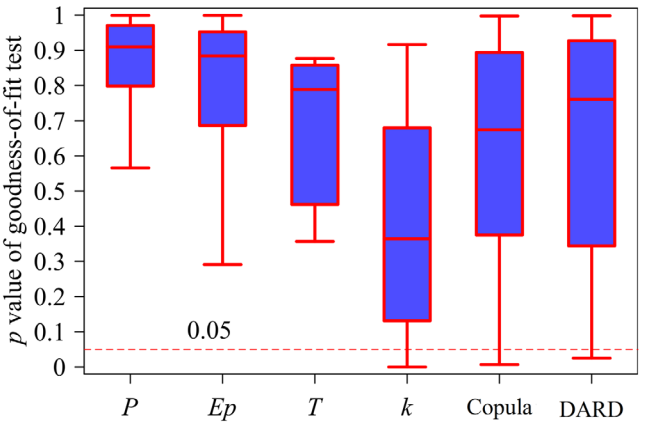

Figure 6. Results of goodness-of-fit test for marginal distributions for (*P*,*Ep*,*T*,*k*), pair copula, and the DARD. The *p* value smaller than 0.05 indicates a poor fit.

divided by the long-term mean of observed annual runoff. The linear trends of the means of the DARDs show a general consistency with the linear trends of the observed runoffs for most study watersheds.

3.5. Nonstationarity Scenario Identification for the DARD

In section 2.1, the four different scenarios in causing the nonstationarities of the derived runoff distribution have been discussed based on equation (2). For each watershed, the nonstationarity scenario of the DARD is identified according to the results of the nonstationary analysis for both the hydrological inputs (Table 3) and Fu-equation parameter *w* (Table 2), and then is displayed in Figure 8. For most watersheds in the Yangtze River basin, scenarios 1 and 2 prevail, while for the Yellow River basin, scenarios 1 and 3 prevail.

For each of the four nonstationarity scenarios, a typical watershed is selected, and then the time variations of five different quantiles of the DARD are plotted in Figure 9. To see how the nonstationarity of the DARD is linked to the corresponding drivers, the time variations of the annual precipitation, potential evaporation, and Fu-equation parameter *w* are also presented. If the covariates of *w* include only the human activity indices (such as Figure 9a) or *w* is a constant (such as Figure 9b), the line for *w* is therefore a smooth line, which should be an intuitive presentation for the variation of *w*. While if the covariates of *w* include at least one climatic variable, the line for *w* should be a wavy line following the climatic covariate (such as Figures 9c and 9d). For a clearer presentation of the evolution of *w*, the mean value of *w* is calculated using equation (13) by replacing the climatic covariate by its mean, and then is displayed by a dashed line.

From the quantile plots for the Hengjiang watershed as displayed in Figure 9a, the mean of the DARD exhibits a decreasing trend as well as an abrupt decline in 1986. This can be explained by Figure 9a, where the mean of annual precipitation in this watershed has a downward abrupt change from 843.3 to 750.5 mm in 1986, and *w* presents an increasing trend along with population growth. As shown by the quantile plot in Figure 9b, the mean of the DARD for the Fushun watershed has a continuous decreasing trend throughout the whole observation period, and a slight downward abrupt change occurs in 2000. This can be linked to the decreasing trend in precipitation and the abrupt increase in potential evaporation, respectively. It should be noted that the precipitation decrease is the primary driver reducing the annual runoff. The quantile plot in Figure 9c indicates that the mean of the DARD for the Huaxian watershed presents a decreasing trend in the observation period. From Figure 9c, the hydrological inputs of both precipitation and potential evaporation in the Huaxian watershed are stationary, while *w* for this watershed is positively related to population and therefore has an increasing trend. Hence, human activities should be responsible for the decline in the annual runoff of the Huaxian watershed. Figure 9d indicates that the DARD

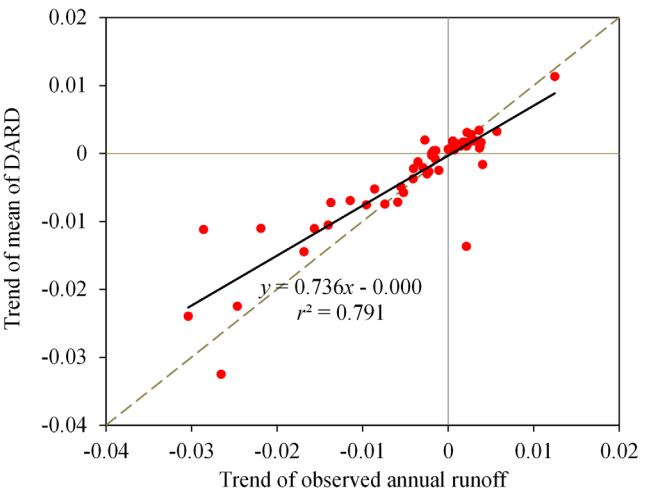

Figure 7. Comparison between the trends of the observed annual runoff and the mean of the DARD.

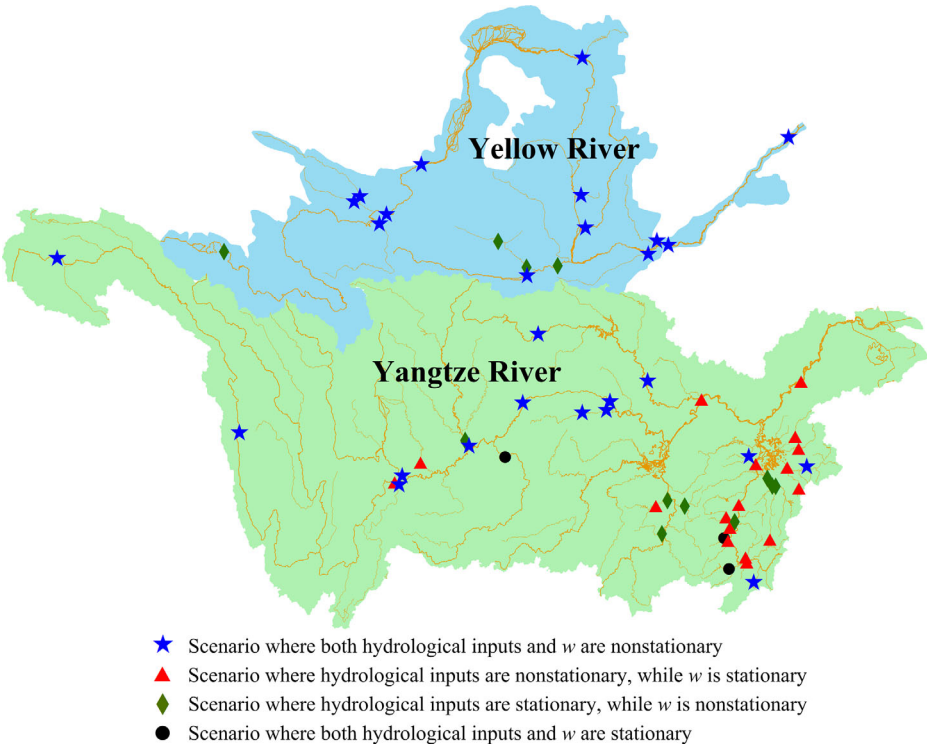

Figure 8. Nonstationarity scenario identification for the DARD for each watershed.

of the Wulong watershed is stationary, since both the hydrological inputs and w for this watershed follow stationary processes. It should be noticed that w is not a constant but it still follows a stationary process, since its covariate precipitation is stationary.

3.6. Difference in the Nonstationarity Identification for Annual Runoff Between the DARD and Trend/Change-Point Tests

In section 3.5, the annual runoff nonstationarity is identified by the DARD with linking to the nonstationarities of both the hydrological inputs and Fu-equation parameter w (see Figure 8). Figure 5a also displays the results of annual runoff nonstationarity identification by the trend/change-point tests. From Figures 5a and 8, it is found that the DARDs are always nonstationary for these watersheds, where the trend/change-point tests indicate the nonstationarity in the observed annual runoff series. While for many other study watersheds, the DARD and trend/change-point tests obtain the different nonstationarity identifications for the annual runoff that, the trend/change-point tests indicate no detectable nonstationarity in the observed runoff, while the DARD proves to be nonstationarity. Typically, for the Datong and Loujiacun watersheds from the Yangtze River shown in Figure 10, despite that their observed annual runoffs are identified as stationary by trend/change-point tests, the DARDs are nonstationary because of the nonstationarities in hydrological inputs or the Fu-equation parameter w. These findings above indicate that the runoff change detected by trend/change-point tests can be related to the changes in hydrological inputs or w, but the changes detected in hydrological inputs or w do not necessarily result in a strong detectable change in observed runoff.

4. Discussion

4.1. Impacts of Model Error k on the DARD

In this study, the annual runoff model error k can originate from two potential sources, one is the inappropriate use of the Fu equation to estimate evaporation at the annual scale, and the other is caused by ignoring the interannual change of catchment water storage in the water balance equation. In theory, it would be possible to introduce an explicit representation of the catchment water storage into the annual runoff simulation under the Budyko framework [*Zhang et al.*, 2008; *Wang*, 2012]. Adding the term of interannual

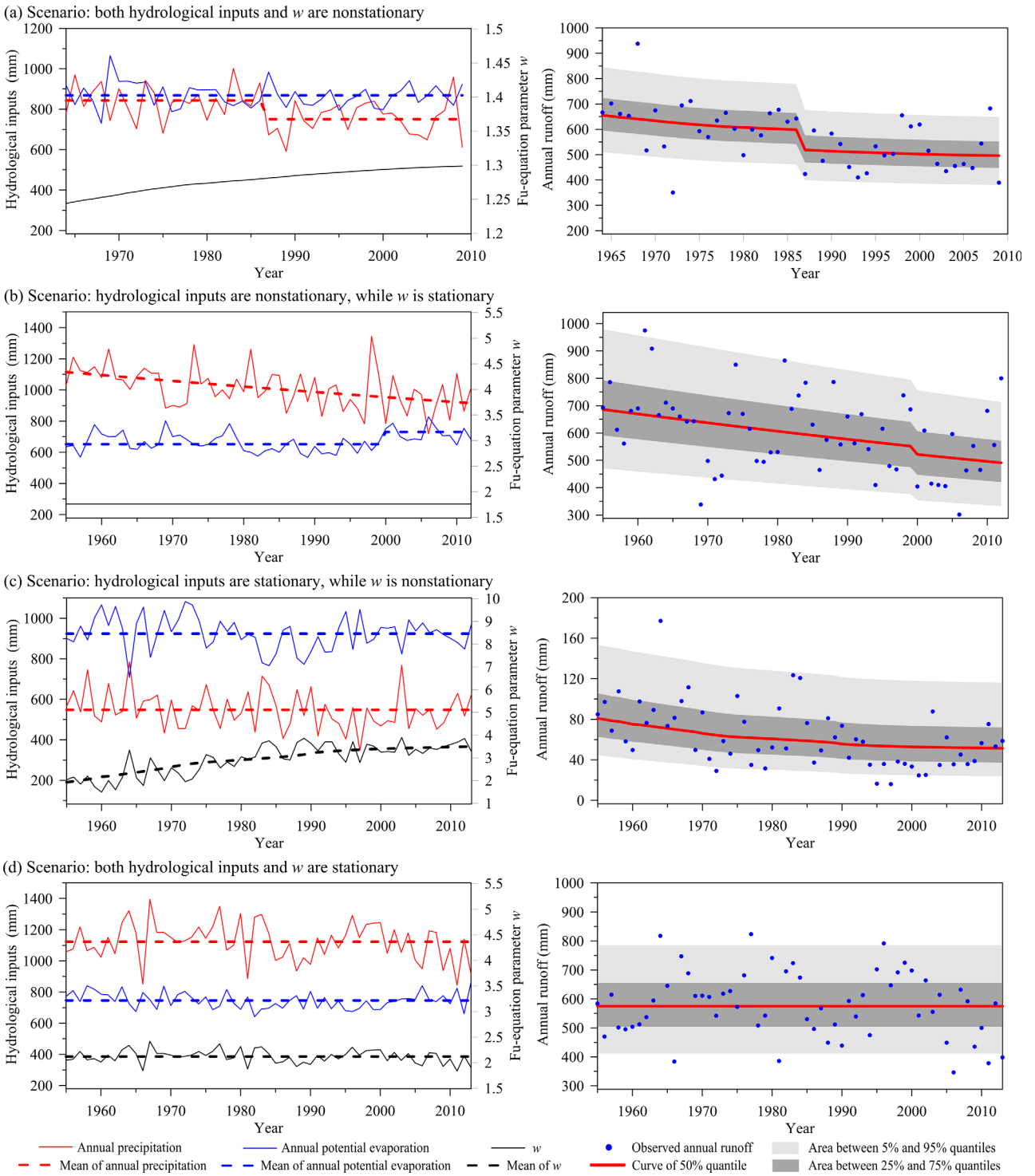

Figure 9. Evolutions of hydrological inputs and the Fu-equation parameter *w* (left column), as well as the quantile plot of the DARD (right column) for the typical watershed belonging to each nonstationarity scenario. (a) Hengjiang watershed; (b) Fushun watershed; (c) Huaxian watershed; (d) Wulong watersheds. The Hengjiang, Fushun, and Wulong watersheds belong to the Yangtze River basin, while the Huaxian watershed belongs to the Yellow River basin.

change of catchment water storage into the runoff simulation should be helpful to obtain a more accurate estimation for annual runoff [*Wang*, 2012]. However, long-term observed data of the water storage at the catchment scale (such as soil moisture and groundwater level) are usually unavailable in practice. Although the catchment water storage can be alternatively estimated from some monthly or daily hydrological

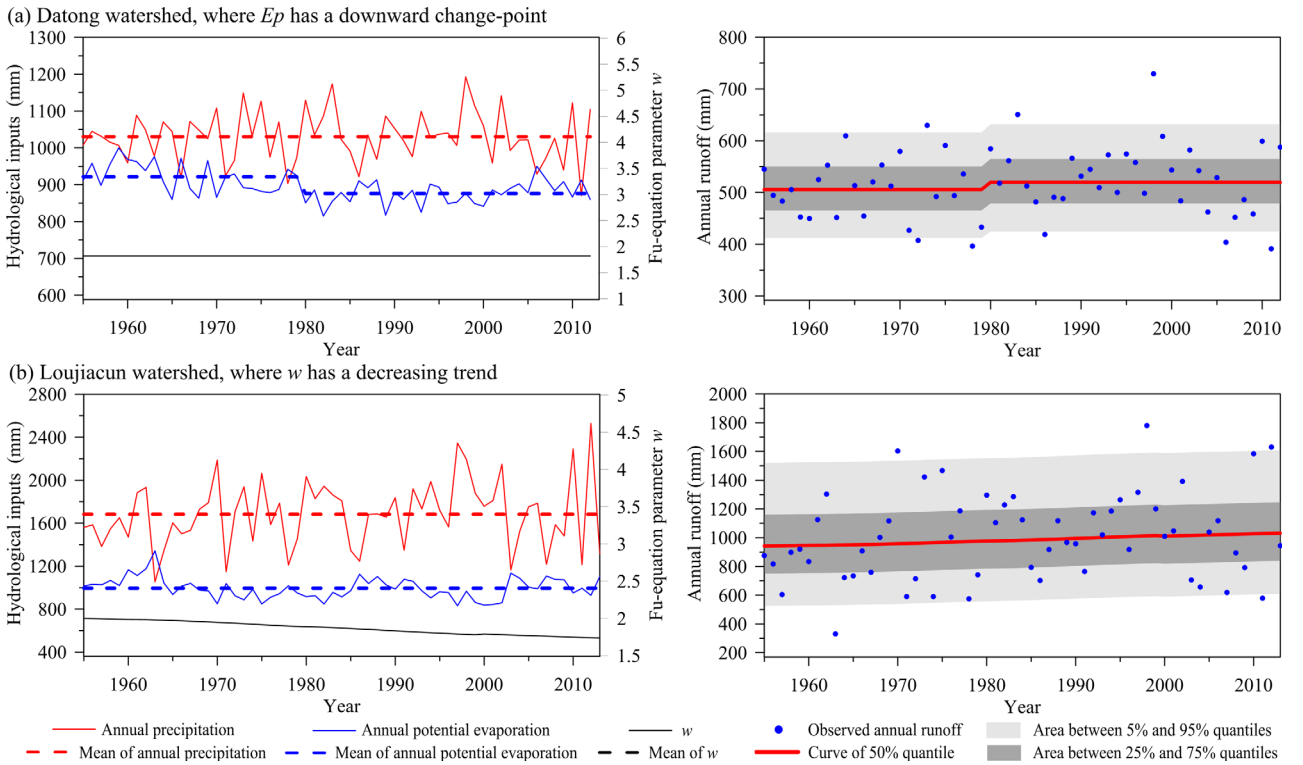

Figure 10. Evolutions of hydrological inputs and the Fu-equation parameter *w* (left column), as well as the quantile plot of the DARD (right column) for the typical watersheds located in the Yangtze River basin, where the hydrological inputs or the Fu-equation parameter *w* are nonstationary, while neither significant trend nor change point can be detected in the runoff series.

models, there would remain numerous uncertainties in the estimated values of the catchment water storage. Therefore, we prefer to treat the interannual change of catchment water storage as a part of the total error in annual runoff simulation, and implicitly consider its effect on the DARD via the model multiplicative error *k* instead of using an explicit water storage representation.

The model error has seldom been considered in previous applications of the analytical derivation approach for runoff frequency analysis [*Eagleson*, 1972; *Gottschalk and Weingartner*, 1998; *Fiorentino and Iacobellis*, 2001; *De Michele and Salvadori*, 2002]. Figure 11 compares the performance of the process-based analytical derivation approaches with considering *k* and without considering *k* (i.e., set $k=1$) in estimating the DARD. In terms of the *p* value of the KS test for the DARD, introducing *k* as a random variable is able to significantly

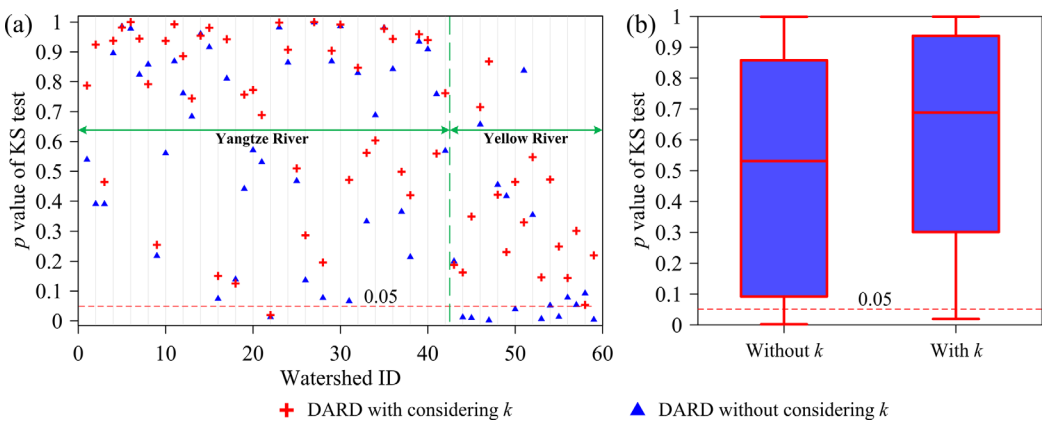

Figure 11. Performance comparison of the DARD with and without considering *k*. (a) Results for each individual watershed; (b) comparison of the overall performance of the DARD.

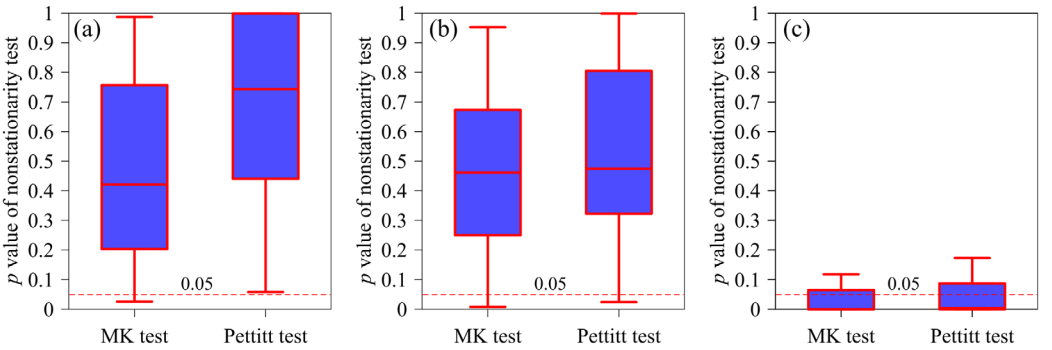

Figure 12. Results of trend and change-point tests for the model error k. Figure 12a is for those watersheds belonging to the nonstationarity scenario 2 or scenario 4, in both of which the Fu-equation parameter w follows a stationary process. Figure 12b is for those watersheds belonging to the nonstationarity scenario 1 or scenario 3, in both of which w follows a nonstationary process. Figure 12c is for those watersheds that belong to the nonstationarity scenario 1 or scenario 3, but the runoffs are simulated by using the annual runoff model with the constant parameter $\bar{w}$.

improve the performance of the process-based analytical derivation approach in fitting annual runoff distribution. Therefore, the model error in runoff simulation should be a factor involved in deriving runoff distribution [*Farmer and Vogel*, 2016]. Similar to the performance of the annual runoff model displayed in Figure 3a, the DARD for the Yangtze River generally has the better fitting effect on the annual runoff distribution than that for the Yellow River. This finding indicates that the performance of the analytical derivation approach is probably related to the simulation accuracy of the annual runoff.

4.2. Nonstationary Behavior of k in Presenting the Nonstationarity of Hydrological Processes

In this study, the model error k is assumed to follow a stationary process when there is no systematic bias in the runoff simulation. From the results of trend/change-point tests displayed in Figures 12a and 12b, k tends to follow a stationary process for most study watersheds no matter whether or not w follows a stationary process. This indicates that sources of the nonstationarity in runoff generation processes have been properly identified. However, if a stationary annual runoff model is used to model the nonstationary runoff generation processes, then the nonstationarity in the runoff generation processes could be transferred to the model error, leading to the nonstationarity of model error k. For example, if the annual runoff model with the constant Fu-equation parameter $\bar{w}$ is employed to simulate the annual runoff of the watersheds belonging to the nonstationarity scenarios 1 and 3, where w has been proven to follow a nonstationary process, then the calibrated value of k tends to present a significant trend or change point (see Figure 12c). The nonstationarity in k might suggest that a source of nonstationarity of the runoff generation processes represented by w has been missed by the annual runoff model with the constant parameter $\bar{w}$.

5. Conclusions

In this paper, we present a process-based approach to analytically derive the nonstationary distribution of annual runoff, with the Fu equation used to represent the annual runoff generation processes. By such an approach, possible causes of the nonstationarity of the annual runoff can be investigated, such as the nonstationarity of hydrological inputs including precipitation and potential evaporation, and the nonstationarity of catchment characteristics, which dominate runoff generation and are represented by the Fu-equation parameter w. Unlike the trend/change-point tests directly applied to the observed runoff data, the proposed nonstationary process-based analytical derivation approach is able to provide a physical insight into the factors related to the nonstationarities of annual runoff distribution.

This process-based approach has been employed to perform nonstationarity analysis for the annual runoff series of 59 watersheds in the Yangtze River basin and Yellow River basin, China. The results indicate that the DARDs for the majority of the study watersheds have a satisfactory performance in fitting the annual runoff distributions. The covariate analysis for the Fu-equation parameter w indicates that the runoff generation processes for the majority of the study watersheds, especially those in the Yellow River basin, have been disturbed either by climate change or by human activities. In general, the DARDs for most study

watersheds are found to be nonstationary, due to the nonstationarities in hydrological inputs (mainly potential evaporation) and/or *w*.

Acknowledgments
This research is supported by the National Natural Science Foundation of China (grant 51525902, 51190094, and 51479139), which are greatly appreciated. Sincere thanks are also due to the Associate Editor and reviewers for their constructive remarks and suggestions that have helped the improvement of the manuscript. The data used in this paper can be requested by contacting the corresponding author L. Xiong at xionglh@whu.edu.cn.

References

Aas, K., C. Czado, A. Frigessi, and H. Bakken (2009), Pair-copula constructions of multiple dependence, *Insur. Math. Econ.*, *44*(2), 182–198, doi:10.1016/j.insmatheco.2007.02.001.

Bender, J., T. Wahl, and J. Jensen (2014), Multivariate design in the presence of non-stationarity, *J. Hydrol.*, *514*, 123–130, doi:10.1016/j.jhydrol.2014.04.017.

Blazkova, S., and K. Beven (1997), Flood frequency prediction for data limited catchments in the Czech Republic using a stochastic rainfall model and TOPMODEL, *J. Hydrol.*, *195*, 256–278.

Blöschl, G., and M. Sivapalan (1997), Process controls on regional flood frequency: Coefficient of variation and basin scale, *Water Resour. Res.*, *33*(12), 2967–2980.

Blöschl, G., et al. (2007), At what scales do climate variability and land cover change impact on flooding and low flows?, *Hydrol. Processes*, *21*, 1241–1247.

Budyko, M. I. (1974), *Climate and Life*, 508 pp., Academic Press, New York.

Burn, D. H., and M. A. Hag Elnur (2002), Detection of hydrologic trends and variability, *J. Hydrol.*, *225*, 107–122, doi:10.1016/S0022-1694(01)00514-5.

Cameron, D., K. Beven, and P. Naden (2000), Flood frequency estimation by continuous simulation under climate change (with uncertainty), *Hydrol. Earth Syst. Sci.*, *4*(3), 393–405, doi:10.5194/hess-4-393-2000.

Cong, Z. T., D. W. Yang, and G. H. Ni (2009) Does evaporation paradox exist in China, *Hydrol. Earth Syst. Sci.*, *13*, 357–366, doi:hydrol-earth-syst-sci.net/13/357/2009/.

Cui, B.-L., and X. Y. Li (2016), The impact of climate changes on water level of Qinghai Lake in China over the past 50 years, *Hydrol. Res.*, *47*(2), 532–542.

De Michele, C., and G. Salvadori (2002), On the derived flood frequency distribution: Analytical formulation and the influence of antecedent soil moisture condition, *J. Hydrol.*, *262*, 245–258, doi:10.1016/S0022-1694(02)00025-2.

Department of Comprehensive Statistics of National Bureau of Statistics (2010), *China Compendium of Statistics 1949 − 2008*, China Stat. Press, Beijing.

Di Baldassarre, G., M. Kooy, J. S. Kemerink, and L. Brandimarte (2013), Towards understanding the dynamic behaviour of floodplains as human-water systems, *Hydrol. Earth Syst. Sci.*, *17*(8), 3235–3244, doi:10.5194/hess-17-3235-2013.

Donohue, R. J., M. L. Roderick, and T. R. McVicar (2010), Can dynamic vegetation information improve the accuracy of Budyko's hydrological model?, *J. Hydrol.*, *390*(1–2), 23–34, doi:10.1016/j.jhydrol.2010.06.025.

Du, T., L. Xiong, C.-Y. Xu, C. J. Gippel, S. Guo, and P. Liu (2015), Return period and risk analysis of nonstationary low-flow series under climate change, *J. Hydrol.*, *527*, 234–250, doi:10.1016/j.jhydrol.2015.04.041.

Eagleson, P. S. (1972), Dynamics of flood frequency, *Water Resour. Res.*, *8*(4), 878–898, doi:10.1029/WR008i004p00878.

Farmer, W. H., and R. M. Vogel (2016), On the deterministic and stochastic use of hydrologic models, *Water Resour. Res.*, *52*, 5619–5633, doi:10.1002/2016WR019129.

Fiorentino, M., and V. Iacobellis (2001), New insights into the climatic and geologic controls on the probability distribution of floods, *Water Resour. Res.*, *37*(3), 721–730.

Frank, J., and J. R. Massey (1951), The Kolmogorov-Smirnov test for goodness of fit, *J. Am. Stat. Assoc.*, *46*(253), 68–78.

Fu, B. P. (1981), On the calculation of the evaporation from land surface (in Chinese), *Sci. Atmos. Sin.*, *5*(1), 23–31.

Gottschalk, L., and R. Weingartner (1998), Distribution of peak flow derived from a distribution of rainfall volume and runoff coefficient, and a unit hydrograph, *J. Hydrol.*, *208*, 148–162.

Hall, J., et al. (2014), Understanding flood regime changes in Europe: A state of the art assessment, *Hydrol. Earth Syst. Sci.*, *18*(7), 2735–2772.

Hundecha, Y., and B. Merz (2012), Exploring the relationship between changes in climate and floods using a model-based analysis, *Water Resour. Res.*, *48*, W04512, doi:10.1029/2011WR010527.

Jiang, C., L. Xiong, C.-Y. Xu, and S. Guo (2015a), Bivariate frequency analysis of nonstationary low-flow series based on the time-varying copula, *Hydrol. Processes*, *29*, 1521–1534, doi:10.1002/hyp.10288.

Jiang, C., L. Xiong, D. Wang, P. Liu, S. Guo, and C.-Y. Xu (2015b), Separating the impacts of climate change and human activities on runoff using the Budyko-type equations with time-varying parameters, *J. Hydrol.*, *522*, 326–338.

Kendall, M. G. (1975), *Rank Correlation Measures*, Charles Griffin, London.

Kim, K. B., H.-H. Kwon, and D. W. Han (2016), Hydrological modelling under climate change considering nonstationarity and seasonal effects, *Hydrol. Res.*, *47*(2), 260–273.

Kumar, S., F. Zwiers, P. A. Dirmeyer, D. M. Lawrence, R. Shrestha, and A. T. Werner (2016), Terrestrial contribution to the heterogeneity in hydrological changes under global warming, *Water Resour. Res.*, *52*, 3127–3142, doi:10.1002/2016WR018607.

Li, D., M. Pan, Z. Cong, L. Zhang, and E. Wood (2013), Vegetation control on water and energy balance within the Budyko framework, *Water Resour. Res.*, *49*, 969–976, doi:10.1002/wrcr.20107.

Li, H., S. Beldring, and C.-Y. Xu (2015), Stability of model performance and parameter values on two catchments facing changes in climatic conditions, *Hydrol. Sci. J.*, *60*(7–8), 1317–1330, doi:10.1080/02626667.2014.978333.

López, J., and F. Francés (2013), Non-stationary flood frequency analysis in continental Spanish rivers, using climate and reservoir indices as external covariates, *Hydrol. Earth Syst. Sci.*, *17*, 3189–3203, doi:10.5194/hess-17-3189-2013.

Mann, H. B. (1945), Non-parametric tests against trend, *Econometrica*, *13*, 245–259.

McMillan, H., et al. (2016), Panta Rhei 2013–2015: Global perspectives on hydrology, society and change, *Hydrol. Sci. J.*, *61*(7), 1174–1191, doi:10.1080/02626667.2016.1159308.

Merz, B., S. Vorogushyn, S. Uhlemann, J. Delgado, and Y. Hundecha (2012), HESS opinions "More efforts and scientific rigour are needed to attribute trends in flood time series," *Hydrol. Earth Syst. Sci.*, *16*(5), 1379–1387, doi:10.5194/hess16-1379-2012.

Merz, B., S. Vorogushyn, U. Lall, A. Viglione, and G. Bloschl (2015), Charting unknown waters—On the role of surprise in flood risk assessment and management, *Water Resour. Res.*, *51*, 6399–6416, doi:10.1002/2015WR017464.

Merz, R., and G. Blöschl (2009a), A regional analysis of event runoff coefficients with respect to climate and catchment characteristics in Austria, *Water Resour. Res.*, *45*, W01405, doi:10.1029/2008WR007163.

Merz, R., and G. Blöschl (2009b), Process controls on the statistical flood moments—A data based analysis, *Hydrol. Processes*, *23*, 675–696.

Merz, R., J. Parajka, and G. Blöschl (2011), Time stability of catchment model parameters: Implications for climate impact analyses, *Water Resour. Res.*, *47*, W02531, doi:10.1029/2010WR009505.
Montanari, A., and D. Koutsoyiannis (2012), A blueprint for process-based modeling of uncertain hydrological systems, *Water Resour. Res.*, *48*, W09555, doi:10.1029/2011WR011412.
Montanari, A., and D. Koutsoyiannis (2014), Modeling and mitigating natural hazards: Stationarity is immortal!, *Water Resour. Res.*, *50*, 9748–9756, doi:10.1002/2014WR016092.
Montanari, A., et al. (2013), "Panta Rhei—Everything flows": Change in hydrology and society—The IAHS scientific decade 2013–2022, *Hydrol. Sci. J.*, *58*(6), 1256–1275, doi:10.1080/02626667.2013.809088.
Nash, J. E., and J. V. Sutcliffe (1970), River flow forecasting through conceptual models, *J. Hydrol.*, *10*, 282–290.
Nelsen, R. B. (2006), *An Introduction to Copulas*, Springer, New York.
Pathiraja, S., L. Marshall, A. Sharma, and H. Moradkhani (2016), Hydrologic modeling in dynamic catchments: A data assimilation approach, *Water Resour. Res.*, *52*, 3350–3372, doi:10.1002/2015WR017192.
Pettitt, A. N. (1979), A non-parametric approach to the change-point problem, *Appl. Stat.*, *28*, 126–135.
Rahman, A., P. E. Weinmann, T. M. T. Hoang, and E. M. Laurenson (2002), Monte Carlo simulation of flood frequency curves from rainfall, *J. Hydrol.*, *256*, 196–210.
Read, L. K., and R. M. Vogel (2016), Hazard function analysis for flood planning under nonstationarity, *Water Resour. Res.*, *52*, 4116–4131, doi:10.1002/2015WR018370.
Rogger, M., B. Kohl, H. Pirkl, A. Viglione, J. Komma, R. Kirnbauer, R. Merz, and G. Blöschl (2012a), Runoff models and flood frequency statistics for design flood estimation in Austria: Do they tell a consistent story?, *J. Hydrol.*, *456–457*, 30–43, doi:10.1016/j.jhydrol.2012.05.068.
Rogger, M., H. Pirkl, A. Viglione, J. Komma, B. Kohl, R. Kirnbauer, R. Merz, and G. Blöschl (2012b), Step changes in the flood frequency curve: Process controls, *Water Resour. Res.*, *48*, W05544, doi:10.1029/2011WR011187.
Rogger, M., A. Viglione, J. Derx, and G. Blöschl (2013), Quantifying effects of catchments storage thresholds on step changes in the flood frequency curve, *Water Resour. Res.*, *49*, 6946–6958, doi:10.1002/wrcr.20553.
Salas, J. D., and J. Obeysekera (2014), Revisiting the concepts of return period and risk for nonstationary hydrologic extreme events, *J. Hydrol. Eng.*, *19*(3), 554–568, doi:10.1061/(ASCE)HE.1943-5584.0000820.
Schwarz, G. (1978), Estimating the dimension of a model, *Ann. Stat.*, *6*(2), 461–464.
Sivapalan, M., and G. Blöschl (2015), Time scale interactions and the coevolution of humans and water, *Water Resour. Res.*, *51*, 6988–7022, doi:10.1002/2015WR017896.
Sivapalan, M., G. Blöschl, R. Merz, and D. Gutknecht (2005), Linking flood frequency to long-term water balance: Incorporating effects of seasonality, *Water Resour. Res.*, *41*, W06012, doi:10.1029/2004WR003439.
Sivapalan, M., H. H. G. Savenije, and G. Blöschl (2012), Socio-hydrology: A new science of people and water, *Hydrol. Processes*, *26*, 1270–1276.
Stocker, T. F., D. Qin, G.-K. Plattner, M. Tignor, S. K. Allen, J. Boschung, A. Nauels, Y. Xia, V. Bex, and P. M. Midgley (Eds.) (2013), *Climate Change 2013: The Physical Science Basis. Contribution of Working Group I to the Fifth Assessment Report of the Intergovernmental Panel on Climate Change*, Cambridge Univ. Press, Cambridge.
Strupczewski, W. G., V. P. Singh, and W. Feluch (2001), Non-stationary approach to at-site flood frequency modeling I. Maximum likelihood estimation, *J. Hydrol.*, *248*, 123–142, doi:10.1016/S0022-1694(01)00397-3.
Turner, S. W. D., and S. Galelli (2016), Regime-shifting streamflow processes: Implications for water supply reservoir operations, *Water Resour. Res.*, *52*, 3984–4002, doi:10.1002/2015WR017913.
Villarini, G., F. Serinaldi, J. A. Smith, and W. F. Krajewski (2009), On the stationarity of annual flood peaks in the Continental United States during the 20th Century, *Water Resour. Res.*, *45*, W08417, doi:10.1029/2008WR007645.
Vogel, R. M., C. Yaindl, and M. Walter (2011), Nonstationarity: Flood magnification and recurrence reduction factors in the United States, *J. Am. Water Resour. Assoc.*, *47*(3), 464–474, doi:10.1111/j.1752-1688.2011.00541.x.
Vogel, R. M., A. Rosner, and P. H. Kirshen (2013), Brief communication: Likelihood of societal preparedness for global change: Trend detection, *Nat. Hazards Earth Syst. Sci.*, *13*, 1–6.
Vogel, R. M., U. Lall, X. Cai, B. Rajagopalan, P. K. Weiskel, R. P. Hooper, and N. C. Matalas (2015), Hydrology: The interdisciplinary science of water, *Water Resour. Res.*, *51*, 4409–4430, doi:10.1002/2015WR017049.
Wang, D. (2012), Evaluating interannual water storage changes at watersheds in Illinois based on long-term soil moisture and groundwater level data, *Water Resour. Res.*, *48*, W03502, doi:10.1029/2011WR010759.
Wang, D, and M. Hejazi (2011), Quantifying the relative contribution of the climate and direct human impacts on mean annual streamflow in the contiguous United States, *Water Resour. Res.*, *47*, W00J12, doi:10.1029/2010WR010283.
Wei, Q., C. H. Sun, G. H. Wu, and L. Pan (2016), Haihe River discharge to Bohai Bay, North China: Trends, climate, and human activities, *Hydrol. Res.*, doi:10.2166/nh.2016.142, in press.
Westra, S., M. Thyer, M. Leonard, D. Kavetski, and M. Lambert (2014), A strategy for diagnosing and interpreting hydrological model nonstationarity, *Water Resour. Res.*, *50*, 5090–5113, doi:10.1002/2013WR014719.
Williams, C. A., et al. (2012), Climate and vegetation controls on the surface water balance: Synthesis of evapotranspiration measured across a global network of flux towers, *Water Resour. Res.*, *48*, W06523, doi:10.1029/2011WR011586.
Xiong, L., and S. Guo (2004), Trend test and change-point detection for the annual discharge series of the Yangtze River at the Yichang hydrological station, *Hydrol. Sci. J.*, *49*(1), 99–112, doi:10.1623/hysj.49.1.99.53998.
Xiong, L., and S. Guo (2012), Appraisal of Budyko formula in calculating long-term water balance in humid watersheds of southern China, *Hydrol. Processes*, *26*, 1370–1378.
Xiong, L., K. Yu, and L. Gottschalk (2014), Estimation of the distribution of annual runoff from climatic variables using copulas, *Water Resour. Res.*, *50*, 7134–7152, doi:10.1002/2013WR015159.
Xiong, L., C. Jiang, C.-Y. Xu, K.-X. Yu, and S. Guo (2015), A framework of changepoint detection for multivariate hydrological series, *Water Resour. Res.*, *51*, 8198–8217, doi:10.1002/2015WR017677.
Xu, C.-Y., L. Gong, T. Jiang, and D. Chen (2006), Decreasing reference evapotranspiration in a warming climate—A case of Changjiang (Yangtze River) catchment during 1970–2000, *Adv. Atmos. Sci.*, *23*(4), 513–520.
Yan, R. H., J. C. Huang, Y. Wang, J. F. Gao, and L. Y. Qi (2016), Modeling the combined impact of future climate and land use changes on streamflow of Xinjiang Basin, China, *Hydrol. Res.*, *47*(2), 356–372.
Yang, D. W., W. W. Shao, P. J. F. Yeh, H. B. Yang, S. Kanae, and T. Oki (2009), Impact of vegetation coverage on regional water balance in the nonhumid regions of China, *Water Resour. Res.*, *45*, W00A14, doi:10.1029/2008WR006948.
Yu, K.-X., L. Xiong, and L. Gottschalk (2014), Derivation of low flow distribution functions using copulas, *J. Hydrol.*, *508*, 273–288, doi:10.1016/j.jhydrol.2013.09.057.

Yu, K.-X., L. Gottschalk, L. Xiong, Z. Li, and P. Li (2015), Estimation of the annual runoff distribution from moments of climatic variables, *J. Hydrol.*, *531*, 1081–1094, doi:10.1016/j.jhydrol.2015.11.012.

Yue, S., P. Pilon, and G. Cavadias (2002), Power of the Mann–Kendall and Sperman's rho tests for detecting monotonic trends in hydrological series, *J. Hydrol.*, *259*, 254–271, doi:10.1016/S0022-1694(01)00594-7.

Zhang, L., W. R. Dawes, and G. R. Walker (2001), Response of mean annual evapotranspiration to vegetation changes at catchment scale, *Water Resour. Res.*, *37*(3), 701–708.

Zhang, L., N. Potter, K. Hickel, Y. Zhang, and Q. Shao (2008), Water balance modeling over variable time scales based on the Budyko framework––Model development and testing, *J. Hydrol.*, *360*, 117–131.

Zhang, Z. X., Chen, C.-Y. Xu, L. Yuan, B. Yong, and S. Yan (2011), Evaluating the non-stationary relationship between precipitation and streamflow in nine major basins of China during the past 50 years, *J. Hydrol.*, *409*, 81–93, doi:10.1016/j.jhydrol.2011.07.041.